Computers, Materials & Continua CMC, vol.64, no.1, pp.97-144, 2020

Aspects of Fretting Fatigue Finite Element Modelling

Kyvia Pereira[1], Libardo V. Vanegas-Useche[2] and Magd Abdel Wahab[3, 4, *]

Abstract: Fretting fatigue is a type of failure that may affect various mechanical components, such as bolted or dovetail joints, press-fitted shafts, couplings, and ropes. Due to its importance, many researchers have carried out experimental tests and analytical and numerical modelling, so that the phenomena that govern the failure process can be understood or appropriately modelled. Consequently, the performance of systems subjected to fretting fatigue can be predicted and improved. This paper discusses different aspects related to the finite element modelling of fretting fatigue. It presents common experimental configurations and the analytical solutions for cylindrical contact. Then, it discusses aspects of fretting fatigue crack initiation, such as crack location, orientation, and length, as well as stress averaging approaches. Then, it deals with the propagation stage; crack face interaction, orientation criteria, and crack growth rate are discussed. Lastly, additional aspects of recent research on fretting fatigue are reviewed: out-of-phase loading, cohesive zone modelling, wear effects, heterogeneity, and crystal orientation. Fretting fatigue is a phenomenon not well understood, and much more research is needed so that its understanding is increased and proper criteria and laws may be available for different cases.

Keywords: Fretting fatigue, FEM, modelling, crack initiation, crack growth.

1 Introduction

Fretting is a phenomenon that happens when two surfaces in contact are subjected to oscillatory relative sliding of small amplitude, generally in the range [5, 100] μm [Ding, Leen and McColl (2004)], but it can be smaller. It is observed in many mechanical systems, e.g., press-fitted shafts, dovetail joints, and bearings, or more generally in service conditions where components may be susceptible to vibration, causing alternating sliding movement between the contacting surfaces. Fretting is an important issue, as it may reduce considerably the lifetime of a part by fatigue, wear, or both.

Fretting may have a major influence on the contacting bodies, leading to catastrophic failure.

[1] Soete Laboratory, Faculty of Engineering and Architecture, Ghent University, Zwijnaarde, B-9052, Belgium.

[2] Facultad de Ingeniería Mecánica, Universidad Tecnológica de Pereira, Pereira, 660003, Colombia.

[3] Division of Computational Mechanics, Ton Duc Thang University, Ho Chi Minh, Vietnam.

[4] Faculty of Civil Engineering, Ton Duc Thang University, Ho Chi Minh, Vietnam.

[*] Corresponding Author: Magd Abdel Wahab. Email: magd.abdelwahab@tdtu.edu.vn.

Received: 22 January 2020; Accepted: 15 April 2020.

This may occur by crack nucleation and growth, i.e., fretting fatigue, by material removal due to fretting wear, which may produce loss of fit, or by both phenomena. The type of failure depends primarily on the fretting regime. Vingsbo et al. [Vingsbo and Söderberg (1988)] used a fretting map to describe the behaviour of wear volume and fatigue lifetime as functions of slip displacement for the three fretting regimes, namely gross slip, stick, and partial slip, as shown in Fig. 1. At stick condition, surfaces are considered to be stuck to each other, and no visible damage is generated. As the slip displacement increases in the mixed stick-slip condition, the fatigue life decreases and the wear rate remains reasonably low. Thus, the main failure mechanism in this regime is fretting fatigue. For even higher slip displacements, the regime changes to gross slip condition, where the wear rate increases considerably. Fretting fatigue is not significant at this regime, because the cracks nucleated are removed by the intense amount of wear. In addition, the redistribution of contact stresses reduces sub-surface stresses [Cardoso, Doca, Néron et al. (2019)].

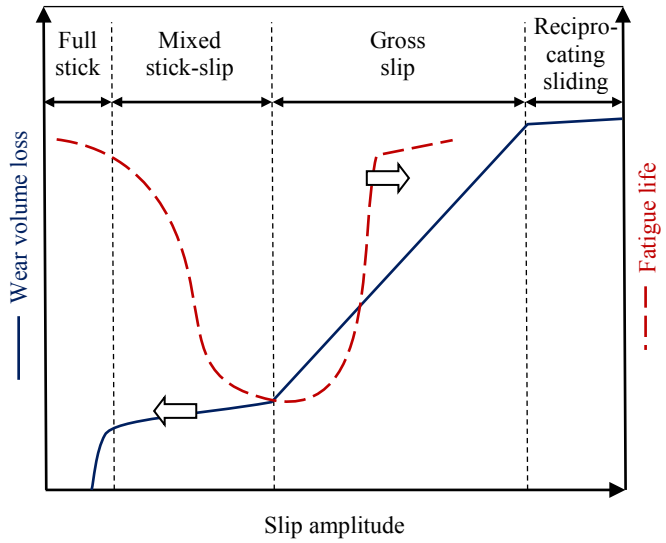

Figure 1: Fretting map proposed by Vingsbo et al. [Vingsbo and Söderberg (1988)]

As discussed by Dobromirski [Dobromirski (1992)], although up to 50 variables might impact the fretting process, it is possible to identify a set of "primary" and "secondary" fretting variables that govern the phenomenon. The "primary" set is composed of the Coefficient of Friction (COF), slip amplitude, and contact pressure. The "secondary" set consists of the variables that impact the "primary" set, causing an indirect impact on fretting.

Several laboratory tests are commonly utilised, mainly full scale and coupon tests, to study the effects of those variables. Full-scale tests replicate real service conditions and components. For instance, some researchers [Golden and Nicholas (2005); Conner and Nicholas (2006); Golden (2009)] studied the phenomenon considering test set-ups that mimic dovetails joints. Bolted or riveted lap joints are also common assemblies that are studied in full scale tests [Chakherlou, Mirzajanzadeh and Vogwell (2009); Eriten, Polycarpou and Bergman (2011); Oskouei and Ibrahim (2012); Ferjaoui, Yue, Abdel Wahab et al. (2015)].

The coupon tests consist of pads that are pressed onto a flat specimen by means of a normal force F. An oscillatory bulk stress $\sigma_{bulk,}$ also referred to as axial load σ_{axial}, is applied to the specimen at one end, whereas the other end is fixed. On the one hand, the typical test configurations may be divided into three main categories (Fig. 2). The first type (a) does not provide any control of the tangential loading applied to the contact interface; only the normal load is maintained through a proving ring. In the second type (b), the use of compliance springs provides an alternative to obtain the tangential loading based on the bulk load and normal load. However, it still does not provide control over the applied tangential load amplitude. The third type (c) makes use of individual actuators to apply the bulk stress and tangential loading, providing full control of the applied loads.

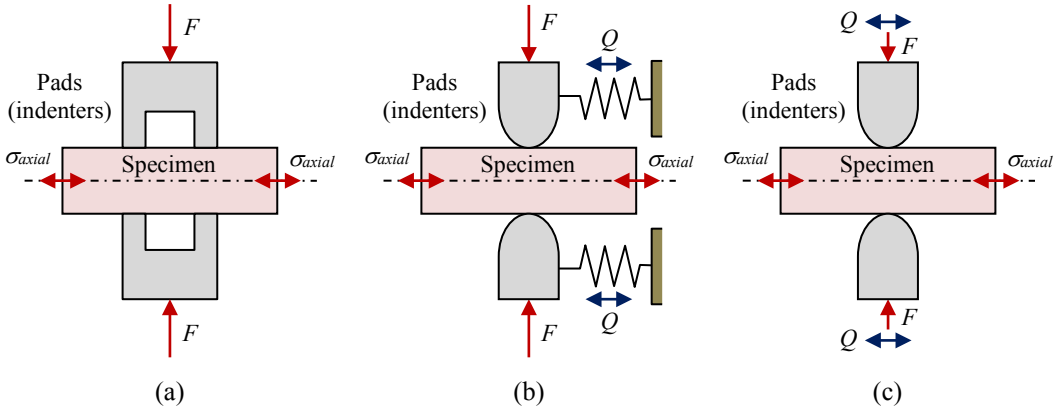

Figure 2: Fretting coupon scale test set-ups: (a) no controlling of slip; (b) indirect information of slip amplitude, through the compliance springs; (c) full control of the applied slip (or tangential) load

On the other hand, the test configurations may be classified according to the shape of the pad. For example, cylinder-on-plane (cases (b) and (c) in Fig. 2), sphere-on-plane, and plane-on-plane (Fig. 2(a)) are commonly used. Most of the works on fretting fatigue deal with cylinder-flat and flat-flat contacts, whereas less research is devoted to spherical contact.

Also, contact problems may be classified as Hills et al. [Hills and Dini (2016)]: incomplete, complete, receding, and common edge. Incomplete contact occurs, e.g., between a cylinder and a plane (as in cases (b) and (c) in Fig. 2). Complete contact takes place when the pad surface is planar and makes full contact with the specimen. Receding contact may be exhibited when the pad is a strip and a central load is applied to it; initially there is full contact, but the load may cause the pad extremes to lose contact. Lastly, common edge is when the pad and the specimen have the same width; therefore, stress singularity at the edges is not exhibited.

Apart from the experimental research, numerical modelling, in particular finite element modelling, is a powerful technique that may be used to analyse fretting, especially for complex geometries, but also to obtain details of the mechanics of fretting. Consequently, the Finite Element Method (FEM) has been widely used to analyse fretting fatigue. Within these analyses, stresses and strains, but also fracture mechanics parameters, such

as the Stress Intensity Factors (SIFs), the energy release rate, and the J-Integral, are of importance. In particular, Linear Elastic Fracture Mechanics (LEFM) is an important approach for fretting fatigue analyses for the crack propagation phase.

In this article we discuss different aspects associated with the modelling of fretting fatigue and review recent research related to it. Section 2 describes analytical solutions for cylindrical contact. Section 3 deals with aspects of fretting fatigue crack nucleation, such as crack location, orientation, and length. Also, some papers dealing with out-of-phase loading and stress averaging for crack initiation analyses are reviewed. Then, aspects of the propagation stage, such as crack face contact, crack orientation criteria, and crack propagation rate are discussed in Section 4. Additional aspects of fretting fatigue modelling, such as cohesive zone model, the influence of wear, heterogeneity, and crystal orientation are reviewed in Section 5. Lastly, some conclusions are provided.

2 Stress analysis

2.1 Overview

This section focuses on fretting fatigue analytical solutions for cylindrical contact, particularly, the contact interface of a cylinder and a plane, representing the usual cylinder-on-plane fretting fatigue test configuration (see, e.g., Fig. 2(b)). As mentioned earlier, in this configuration two cylindrical pads are kept in contact with a flat specimen by means of a clamping force F. The specimen is clamped at one end and an oscillatory bulk stress σ_{axial} is applied to the other. Due to the oscillatory axial stress, an oscillatory tangential force Q is transmitted to the pads through the compliance springs. This tangential force is usually smaller than the product of the COF μ and the normal force F and, consequently, the contact will have a stick region and a slip zone.

For this cylinder-on-flat setup, the specimen stresses and strains can be determined analytically by classical contact mechanics, as described in Section 2.2. The normal load F produces a pressure distribution $p(x)$ that can be determined through Hertzian solutions (Sections 2.2 and 2.3). The tangential force Q and axial stress σ_{axial} produce a surface shear traction $q(x)$. The stress solutions, when Q and σ_{axial} are added, are presented in Sections 2.4 and 2.5, respectively. The solutions obtained by contact mechanics theory are valid for some conditions, e.g., semi-infinite bodies and idealised loading conditions and elastic properties. This theory is important for some fretting problems, particularly for closed form comparisons with experiments [Sunde, Berto and Haugen (2018)].

2.2 Contact mechanics

Contact mechanics studies the interaction between two bodies that contact each other in one or more points [Johnson (1987)]. It has been widely discussed in the literature, and it dates back to 1880s, in a seminal paper of Hertz [Hertz (1882)]. Hertz studied the contact between two curved surfaces that deform slightly due to imposed loads. His work set the foundations for this field and is now known as classical or Hertzian contact mechanics. This theory applies to non-conforming contact of elastic bodies in which the contact zone is much smaller than the sizes of the bodies (half-space theory) [Sunde, Berto and Haugen (2018)].

Several authors have extended Hertz theory. For example, Cattaneo [Cattaneo (1938)] and Mindlin [Mindlin (1949)] independently included tangential forces that produce partial slip condition. Full sliding terms were superimposed with a modification related to the contact pressure (see Section 2.4). These works were followed by additional generalisations to the Cattaneo-Mindlin problem [Mindlin and Deresiewicz (1953); Hamilton and Goodman (1966)]. Also, Johnson et al. [Johnson, Kendall and Roberts (1971)] extended the non-conforming contact of elastic bodies withstanding very small loads to consider adhesive forces related to free surface energy. However, the adhesion forces analysed are negligible for materials of high elastic moduli, such as ceramics and metals.

This section is mostly centred on Johnson [Johnson (1987)]. For the reader interested in a more general approach, in which near van der Waals or adhesive interactions are considered, we refer to Bradley [Bradley (1932)] and Johnson et al. [Johnson, Kendall and Roberts (1971)], respectively. Also, Sunde et al. [Sunde, Berto and Haugen (2018)] presented a short review of analytical solutions and asymptotic methods for different cases and geometries. Furthermore, a review on the use of asymptotic approaches for fretting fatigue is provided by Hills et al. [Hills and Dini (2016)]. The asymptotic approaches are supposed to apply when there is stress concentration or singularities and, therefore, when Hertzian analyses are not applicable. These are exhibited when the contact edges have small radii (stress concentration) or are very sharp (complete contact that leads to singular stresses).

Consider a two-dimensional (2D) case, in which two smooth cylindrical bodies with parallel axes are in contact due to a normal load F (Fig. 3). Bodies 1 and 2 have curvature radii R_1 and R_2, respectively. The plane x-z is considered the contact plane and the line, perpendicular to the x-y plane, that intercepts the Cartesian coordinate system at O (0,0,0) is considered to be the initial contact line. Due to compression, the "motion" of cylinders 1 and 2 may be represented by displacements δ_1 and δ_2, respectively, with $\delta=\delta_1+\delta_2$ defined as the total approach between the bodies. The surface of each cylinder is subjected to a displacement u_{y1} and u_{y2}. The elastic deformations of the bodies produce a contact area of depth l_c, i.e., the length of the cylinders, and width $2a_c$, where a_c, as may be seen in Fig. 3, is the semi-contact width. The contact area is rectangular and equal to $2a_c \times l_c$.

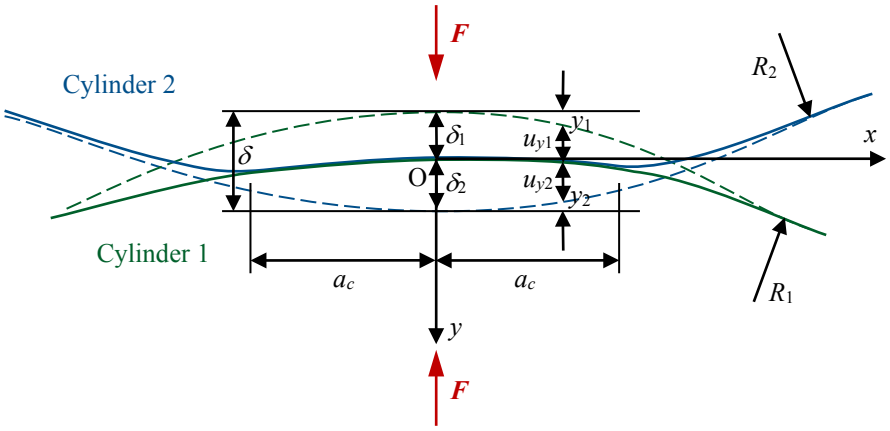

Figure 3: Contact of two cylinders with parallel axes; based on Johnson [Johnson (1987)]

The combined curvature R and combined Young's modulus E^* are given by

$$\frac{1}{R}=\frac{1}{R_1}+\frac{1}{R_2} \tag{1}$$

$$\frac{1}{E^*}=\frac{1-\nu_1^{\,2}}{E_1}+\frac{1-\nu_2^{\,2}}{E_2} \tag{2}$$

where E_i is the modulus of elasticity and v_i is the Poisson's ratio of the ith body (i=1 for body 1 and i=2 for body 2).

The aim here is to obtain the contact pressure distribution $p(x)$ as a function of the coordinate x. However, to do so, the following conditions must be satisfied:

1. The profiles of the surfaces are continuous, smooth, and nonconforming
2. The strains at the contact region are small
3. Near the contact zone, the two parts may be approximated as semi-infinite elastic half-spaces
4. The contact is frictionless

If these assumptions hold, this problem fits into the Hertzian contact mechanics theory, and closed-form expressions for the contact pressure are available, as described beneath.

The displacements u_{y1} and u_{y2} are related to the approach δ by

$$u_{y1}+u_{y2}=\delta-h \tag{3}$$

where h is the separation between the surfaces and is given by h=y_1+y_2. Considering that the cylindrical surfaces are smooth and continuous, h can be re-written as h=x^2/(2R), where x is the Cartesian coordinate measured from point O.

We can differentiate the displacements u_{y1} and u_{y2} with respect to x, obtaining the following surface gradient:

$$\frac{\partial u_{y1}}{\partial x}+\frac{\partial u_{y2}}{\partial x}=-\frac{x}{R} \tag{4}$$

Based on elastic analysis of contact stresses, Johnson [Johnson (1987)] showed that the gradient of the displacements can also be written as function of the contact pressure as

$$\frac{\partial u_{y1}}{\partial x}+\frac{\partial u_{y2}}{\partial x}=-\frac{2}{\pi E^*}\int_{-a_c}^{a_c}\frac{p(s)}{x-s}ds \tag{5}$$

where s is the distance from origin O at contact interface, along the x-axis. Substituting Eq. (5) into Eq. (4) yields:

$$\int_{-a_c}^{a_c}\frac{p(s)}{x-s}ds=-\frac{\pi E^*}{2R}x \tag{6}$$

Solving this integral leads to an elliptical pressure distribution $p(x)$:

$$p(x)=p_{max}\sqrt{1-\left(\frac{x}{a_c}\right)^2}, \quad \text{where} \quad p_{max}=\sqrt{\frac{FE^*}{l_c\pi R}} \tag{7}$$

where p_{max} is the maximum value of the $p(x)$ and is exhibited at the centre of the contact. The force F and the semi-contact width a_c are related:

$$a_c = 2\sqrt{\frac{FR}{l_c \pi E^*}} \tag{8}$$

2.3 Cylindrical contact under normal load

The contact pressure $p(x)$, produced by the normal load F between a cylindrical pad and a flat specimen, can be determined analytically using Eq. (7). For the flat specimen, R_1 becomes infinite and, from Eq. (1), R is equal to the pad radius R_2. As mentioned before, the contact area is rectangular and equal to $2a_c \times l_c$. Fig. 4 illustrates the normalised contact pressure distribution as a function of x/a_c (normalised x-coordinate).

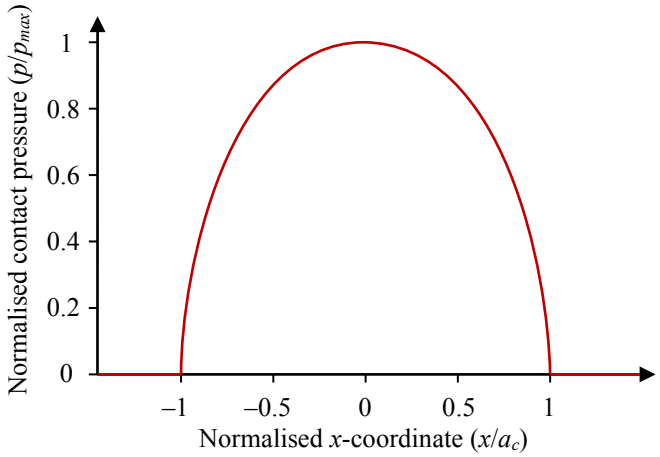

Figure 4: Normalised contact pressure against x/a_c

The subsurface stresses $\sigma_x(y)$ and $\sigma_y(y)$ of the plane x=0 in the x and y directions, respectively, can be written as:

$$\sigma_x(y) = -p_{max}\left[\frac{1+2\left(\frac{y}{a_c}\right)^2}{\sqrt{1+\left(\frac{y}{a_c}\right)^2}} - 2\left|\frac{y}{a_c}\right|\right] \tag{9}$$

and

$$\sigma_y(y) = \frac{-p_{max}}{\sqrt{1+\left(\frac{y}{a_c}\right)^2}} \tag{10}$$

Considering plane strain conditions (no deformation in the z-direction), the stress in the z-direction $\sigma_z(y)$ is correlated to the other components via the Poisson's ratio (ν) of the

planar body: $\sigma_z = \nu(\sigma_x + \sigma_y)$. Therefore, for x=0:

$$\sigma_z(y) = -2\nu\, p_{max}\left[\sqrt{1+\left(\frac{y}{a_c}\right)^2} - \left|\frac{y}{a_c}\right|\right] \tag{11}$$

As an example, considering the case of ν=0.3, the normalised stresses can be plotted as functions of the normalised y-coordinate, as shown in Fig. 5.

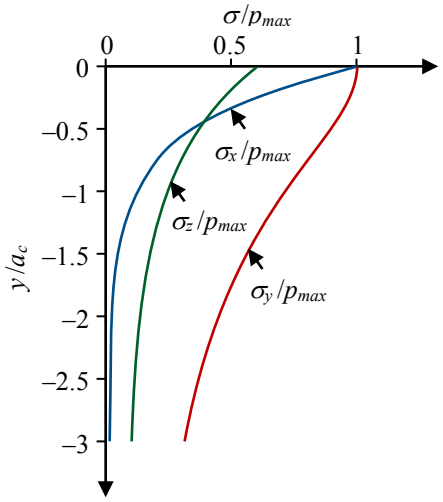

Figure 5: Normalised stresses against the normalised y-coordinate y/a_c

2.4 Cylindrical contact under combined normal and tangential loads

In fretting, the normal force is combined with a tangential friction force Q. To model this case, the Coulomb friction law may be used. Regarding the distribution of the normal pressure $p(x)$, this is the same as in the case of no tangential force, if the two bodies have the same elastic properties [Williams and Dwyer-Joyce (2001)]. However, when they have different elastic constants, shear tractions interact with $p(x)$ and the pressure distribution is not symmetrical [Bufler (1959)]. Nonetheless, the effects of shear tractions are usually minor, particularly for small values of the COF μ; thus, in practice it may be assumed that the distribution of $p(x)$ is the same as in the case of contact without tangential forces [Williams and Dwyer-Joyce (2001)]. Regarding the shear traction on the contact surfaces $q(x)$, it can be modelled as a function of $p(x)$ and the COF. If $Q<\mu F$, the contact area will be have a stick zone and a slip zone; the semi-width of the former zone is symbolised as c. This problem of two cylinders subjected by the forces F and Q such that $Q<\mu F$ is known as the Mindlin problem.

The contact shear traction may be perceived as the sum of two superimposed shear tractions $q'(x)$ and $q''(x)$, as shown in Fig. 6.

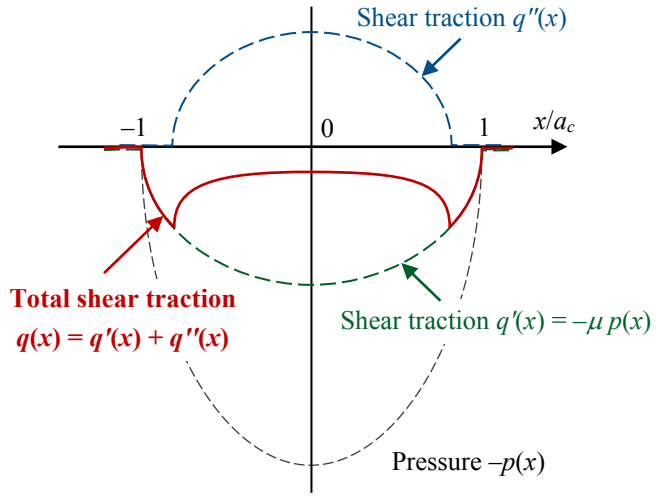

Figure 6: Pressure and shear traction distributions

The shear traction $q(x)$, first found by Cattaneo et al. [Cattaneo (1938); Mindlin (1949)], is given by Nowell et al. [Nowell and Hills (1987)]:

$$q(x) = \begin{cases} -\mu\, p_{max}\sqrt{1-\left(\dfrac{x}{a_c}\right)^2} & \text{if } c \le |x| \le a_c \\ -\mu\, p_{max}\left[\sqrt{1-\left(\dfrac{x}{a_c}\right)^2} - \dfrac{c}{a_c}\sqrt{1-\left(\dfrac{x}{c}\right)^2}\right] & \text{if } |x| < c \end{cases} \quad \text{with} \quad \frac{c}{a_c} = \sqrt{1-\frac{Q}{\mu F}} \qquad (12)$$

2.5 Cylindrical contact under combined normal, tangential, and bulk loads

Nowell et al. [Nowell and Hills (1987)] analysed the effects of bulk stress σ_{axial} on the distributions of stresses. When these bulk stresses are added to the problem, the distribution of the contact shear traction $q(x)$ is eccentric. For the case of a negative value of Q, $q(x)$ is given by Nowell et al. [Nowell and Hills (1987)]:

$$q(x) = \begin{cases} -\mu\, p_{max}\sqrt{1-\left(\dfrac{x}{a_c}\right)^2} & \text{if } c \le |x| \le a_c \\ -\mu\, p_{max}\left[\sqrt{1-\left(\dfrac{x}{a_c}\right)^2} - \dfrac{c}{a_c}\sqrt{1-\left(\dfrac{x-e}{c}\right)^2}\right] & \text{if } |x+e| < c \end{cases} \qquad (13)$$

where

$$\frac{c}{a_c} = \sqrt{1-\frac{Q}{\mu F}} \quad \text{and} \quad e = a_c\frac{\sigma_{axial}}{4\mu\, p_{max}}$$

As an example, Fig. 7 illustrates a distribution of contact shear traction for fretting fatigue

conditions. Based on the distribution of $q(x)$, the peak values of shear tractions and the sizes of the slip and stick zones can be determined.

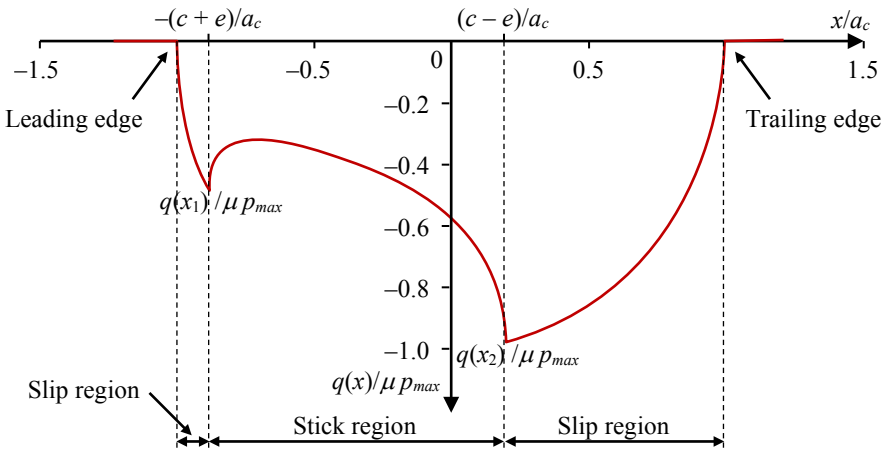

Figure 7: Example of normalised shear stress distribution (μ=0.4, σ_{axial}=100 MPa, Q=155 N, p_{max}=185 MPa, a_c=0.467 mm) [Pereira, Bordas, Tomar et al. (2016)]

Fretting fatigue cracks that may grow until sudden fracture tend to originate at the trailing edge ($x=a_c$) [Hills and Nowell (1994); Lykins, Mall and Jain (2000); Namjoshi, Mall, Jain et al. (2002)], whereas small arrested cracks may initiate near the points of maximum shear traction $q(x_2)$ [Mutoh (1995)]. The trailing edge is the contact edge that is closer to the cyclic bulk load, while the leading edge is closer to the reaction bulk load. The leading crack may initiate at the trailing edge, because of the influence of the tangential stress σ_x on the contact surface: the sharp peak value of this stress $\sigma_{x,max}$, near the contact trailing edge, might play an important role in crack nucleation in fretting fatigue [Szolwinski and Farris (1996)].

Analytical solutions for the elastic normal stress σ_x below the surface are available [Johnson (1987); Hills and Nowell (1994); Szolwinski and Farris (1998)]. Even though bulk stresses make the problem more complex, McVeigh et al. [McVeigh and Farris (1997)] provided a simplified solution for estimating the maximum value of the peak stress $\sigma_{x,max}$ (see Fig. 8):

$$\sigma_{x,max} = 2p_{max}\sqrt{\frac{\mu Q}{F}} + \sigma_{axial} \tag{14}$$

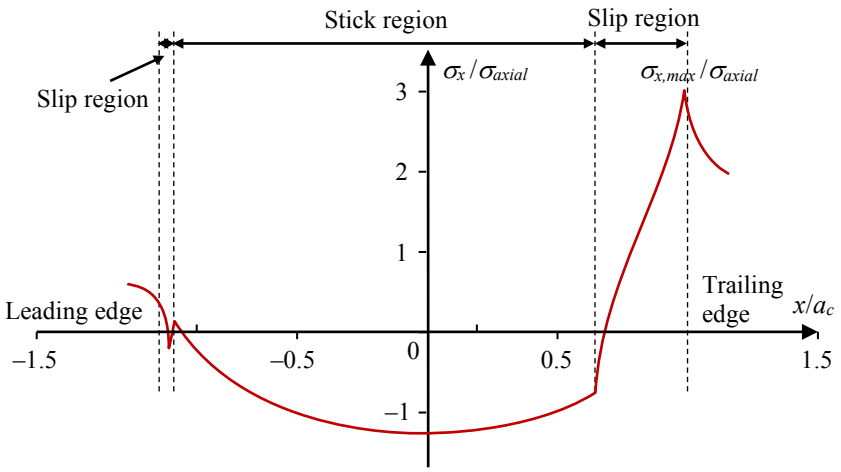

Figure 8: Example of the distribution of the normalised stress σ_x on the contact surface, determined by FEM (μ=0.85, σ_{axial}=100 MPa, Q=155 N, p_{max}=185 MPa, a_c=0.467 mm) [Pereira, Bordas, Tomar et al. (2016)]

Due to the complexity of the fretting phenomenon, analytical solutions are available only for selective situations. These analytical solutions rely on assumptions that are not satisfied in most cases, such as semi-infinite elastic half-space near the contact zone and small strains at contact. In the analytical solution for tangential loading (Eq. (13)), the superimposing of shear stress due to normal load and due to bulk load is a linear approximation and ignores the effect of interaction between both loads. In addition, Eq. (14) is only an approximation of the maximum stress $\sigma_{x,max}$ and may not be representative for all scenarios. Moreover, the stress field near the contact region is variable, multiaxial and non-proportional [Tur, Fuenmayor, Ródenas et al. (2003)], which brings extra complexity to the phenomena. With the advance of computational power, numerical methodologies have become an essential alternative to model fretting without relying on these many assumptions. In this regard, the Finite Element Method (FEM) has been greatly used.

3 Crack initiation

3.1 Overview

Crack initiation or nucleation is an important stage in fretting fatigue, as a large proportion of life is normally spent during initiation. This stage consists in cyclic plastic deformations that eventually result in the formation of a leading crack, usually at the trailing edge of contact. Crack nucleation is highly influenced by the multiaxial non-proportional loading produced by the normal force, the tangential force, and the bulk stress, as described in Sections 1 and 2.

Many studies have already shown that fretting fatigue cracks tend to follow a typical behaviour. In the early 1970s, Wharton et al. [Wharton, Taylor and Waterhouse (1973)] concluded that due to the localised action of fretting, crack nucleates on the surface at

very early stages, in a matter of a few thousand fatigue cycles. At first crack may propagate in the region affected by the contact stresses arising from fretting, in a direction oblique to the surface. Indeed, early fretting fatigue tests have shown that cracks may grow obliquely to the surface at initial stage of propagation [Wharton, Taylor and Waterhouse (1973); Endo and Goto (1976); Nix and Lindley (1988); Conner, Hutson and Chambon (2003)]. Their results also pointed in the direction that as the amplitude of bulk load and slip increase, the combined stresses in the fretting region considerably raise and the fretting-fatigue limit decreases significantly.

Studying carbon steel samples, Endo et al. [Endo and Goto (1976)] also concluded that fretting cracks initiate early in life and that their growth to a certain depth is mainly defined by the combination of tangential (contact) stresses and the repeated axial or bulk load. Their results indicate that shear type cracks are initiated near the contact edge and propagate through a small depth, defined as stage I (initiation stage). Thereafter, stage II (propagation stage, which will be dealt with in Section 4) begins, and the crack grows in a direction oblique to the surface (under mixed-mode) until it reaches a depth large enough, approximately of the order of a few grain sizes. After this point, the effect of contact stresses can be neglected, and the direction of propagation becomes perpendicular to the principal stress of the bulk load. This typical behaviour can be summarised in Fig. 9 and has also been reported over the past thirty years by other researchers testing different materials and fretting conditions [Navarro, Muñoz and Domínguez (2006); Hojjati-Talemi, Abdel Wahab, De Pauw et al. (2014); Cardoso, Araújo, Ferreira et al. (2016)]. However, it has to be mentioned that cracks do not always follow this typical crack growth behaviour. In fact, some researchers have found that cracks may nucleate, for example, perpendicularly to the contact surface, as discussed later.

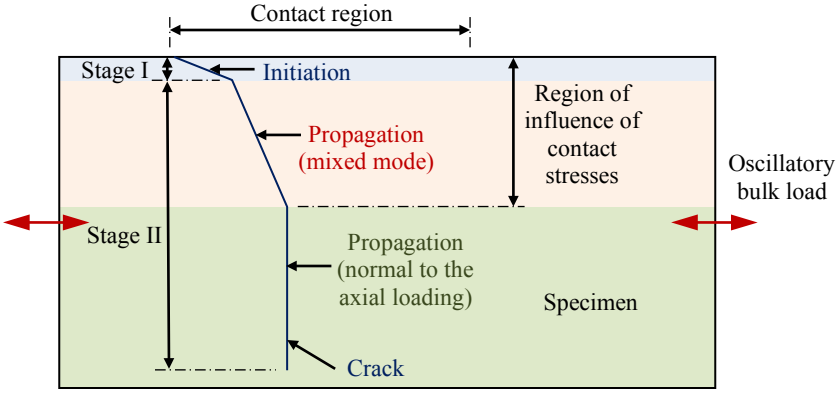

Figure 9: Fretting fatigue crack behaviour

Stage I cracks are considered to be part of the crack initiation phase. At this regime, crack growth is affected by many different factors, such as plasticity, debris, wear [Conner, Hutson and Chambon (2003)], and microstructure. Through metallography and fractography analyses of short cracks (stage I), Nix et al. [Nix and Lindley (1988)] showed a series of parallel ridges running in the direction of growth, suggesting shear mode propagation. Experiments in aluminium and steel by Sato et al. [Sato, Fujii and

Kodama (1986)] showed that crack growth rate in this stage was considerably higher in comparison to plain fatigue. Their results also indicate that in this early stage of propagation, high contact pressures may induce crack closure, which can cause a substantial impact on crack growth rate.

To understand the driving forces for crack initiation is still a research goal [Sunde, Berto and Haugen (2018)], and, accordingly, several criteria and approaches have been used to study this stage. They may be classified as Critical Plane (CP), stress invariant, Continuum Damage Mechanics (CDM), and fretting specific parameters.

In the CP approach, a damage parameter is calculated on a particular plane, i.e., the plane that maximises damage is the critical plane for crack growth. The CP method outperforms the other approaches, as it describes the failure mode, and the orientation of the initiation crack can be determined. However, it tends to use more computational resources, because the damage parameter is calculated for many angles. Regarding the stress invariant method, mostly the Crossland parameter is employed for fretting fatigue, and it is usually used for determining the possibility of crack initiation and its location. The stress invariant approach has the advantage that it might spend less computing time than the CP approach. However, it does not provide information on crack direction. In CDM, a damage variable is defined based on thermodynamic principles; damage nucleation begins at a threshold value, and crack initiates when the damage variable reaches a critical value. The CDM approach is effective to estimate initiation life and location, but it cannot predict crack orientation, as the damage variable is not associated with particular directions. Also, as there is no consensus of a critical value for crack initiation, the limit that separates crack initiation and crack propagation is not unique. The fretting specific parameters, e.g., Ruiz parameters and D_{fret2} [Ding, Sum, Sabesan et al. (2007)] (a modified form of Smith-Watson-Topper (SWT) parameter), may be more appropriate when wear effects are of importance. Ruiz initiation parameter, based on experimental findings, may be employed for determining nucleation location but not for nucleation life and orientation. The D_{fret2} parameter has the advantages that it takes into account the effects of relative slip, it can estimate life accurately, it may provide crack initiation orientation, and it is less computational demanding that wear incremental approaches [Bhatti and Abdel Wahab (2018)].

When comparing life predictions in the literature with experimental data, it can be stated that all methods provide similar degrees of accuracy. Also, there is no approach that produces the best results for all cases, and some significant differences may occur. For example, most of the damage models using CDM assume proportional loading, and this may produce errors, as in fretting fatigue nonproportional loading occurs. Due to the high stress concentrations that are exhibited in some fretting fatigue cases; the accuracy of local damage models depends on stress averaging techniques and the selection of a suitable averaging zone size [Bhatti and Abdel Wahab (2018)].

For the reader interested, further details on these approaches are provided in the comprehensive review of fretting fatigue crack initiation by Bhatti et al. [Bhatti and Abdel Wahab (2018)]. Therefore, this paper does not concentrate on the several approaches and works related to crack initiation, but rather the next subsections present some particularities on crack initiation position, orientation, and length. Stress averaging

techniques and crack initiation analyses for out of phase loading are also reviewed.

3.2 Crack initiation location

In finite element modelling of fretting fatigue, the initial crack is traditionally positioned at the contact edge between the pad and specimen [Giner, Sabsabi, Ródenas et al. (2014); Noraphaiphipaksa, Manonukul, Kanchanomai et al. (2016); De Pannemaecker, Fouvry, Brochu et al. (2016)], where the most severe fretting occurs. Indeed, as discussed by Faanes [Faanes (1995)], the location of the initial crack is (almost) always at the contact edge, as the maximum value of the maximum principal stress occurs there. Furthermore, this is confirmed by many experimental findings [Szolwinski and Farris (1998); Lykins, Mall and Jain (2000); Hojjati-Talemi, Abdel Wahab, De Pauw et al. (2014); Vázquez, Carpinteri, Bohórquez et al. (2019)].

However, many researchers have also attempted to predict its location based on the stress or strain distributions, thermodynamic concepts, and slip at contact interface. For example, Hojjati-Talemi et al. [Hojjati-Talemi and Wahab (2013)] used CDM to study the initiation phase, for cylinder-on-flat, aiming to predict crack initiation lives and location. They suggested that the initial crack location may correspond to the site of the contact region with maximum range of principal strain or the maximum elastic energy density release rate damage criteria. The results for both criteria agree with experimental observations. A drawback of this methodology is the lack of sensitivity regarding changes in the bulk loading.

In a follow up study, Hojjati-Talemi et al. [Hojjati-Talemi, Abdel Wahab, De Pauw et al. (2014)] extended their methodology considering the location being the one that dissipated more energy in one fretting cycle. It was argued that the results, for cylinder-on-plane contact, were in agreement with experimental findings, which indicate that the initiation is at the contact edge. However, the locations predicted for the different cases do not correspond exactly to the contact edge, but they are near to it. Recently, Noraphaiphipaksa et al. [Noraphaiphipaksa, Manonukul and Kanchanomai (2017)] considered different pad geometries (flat and cylindrical) and compared the initial location predicted by two approaches (maximum relative slip amplitude and maximum shear stress range) with experimental data. They concluded that for flat pads, both approaches predict crack location in agreement with laboratory tests. However, for cylindrical pads, the maximum shear stress range method fails to predict the correct location, and the maximum relative slip amplitude is recommended.

The above are just a few examples. The methods that have been proposed to study crack initiation location may be classified as Critical Plane (CP) approaches, stress invariants, fretting specific parameters, and Continuum Damage Mechanics (CDM); all the different methods tend to correlate with experimental findings [Bhatti and Abdel Wahab (2018)]. This is reasonable, as the most severe fretting occurs at the contact edge, and the different criteria and parameters tend to predict initiation location near to it.

3.3 Crack initiation orientation

Depending on the loading conditions, i.e., the relative values of the forces F and Q and

the stress σ_{axial}, a fretting crack may start growing at a small angle, measured from the contact surface, as shown in Fig. 9. Many fretting fatigue tests have shown that crack grows obliquely to the surface [Wharton, Taylor and Waterhouse (1973); Endo and Goto (1976); Nix and Lindley (1988); Szolwinski and Farris (1998); Goh, Wallace, Neu et al. (2001); Conner, Hutson and Chambon (2003); Proudhon, Fouvry and Buffière (2005); Walvekar, Leonard, Sadeghi et al. (2014); Vázquez, Astorga, Navarro et al. (2016)]. When this behaviour is exhibited, crack initiation is controlled by the shear stress range [Giner, Sabsabi, Ródenas et al. (2014)].

However, cracks may initiate at large angles relative to the contact surface and even perpendicular to it. In this case, initiation is dominated by the normal stress range where a large tensile stress is present [Giner, Sabsabi, Ródenas et al. (2014)]. For instance, Vázquez et al. [Vázquez, Carpinteri, Bohórquez et al. (2019)] showed experimentally that crack initiates perpendicular to the contact surface at the trailing edge and then changes direction, inwards at angles of 20° to 28°. The case studied was a cylindrical pad in contact with a flat specimen of aluminium alloy 7075-T651, subjected to a constant pressure and in-phase bulk and tangential loads. Other researchers have also found experimentally that crack initiates nearly normal to the surface [Szolwinski and Farris (1998); Navarro, García and Domínguez (2003)].

According to this, many authors insert the initial crack in a normal direction to the contact surface, perpendicular also to the applied bulk stress, and then evaluate its propagation through the material [Hattori, Nakamura, Sakata et al. (1988); Hills, Nowell and O'Connor (1988); Szolwinski and Farris (1996, 1998); Navarro, García and Domínguez (2003)]. For instance, Hattori et al. [Hattori, Nakamura, Sakata et al. (1988)] used a Finite Element (FE) model to obtain stress distributions at contact interface. Those stresses were later used in junction with fracture mechanics concepts to evaluate Stress Intensity Factors (SIFs), considering that a fretting crack may be approximated by a crack in the edge of a half plane, perpendicular to the surface. Similarly, Hills et al. [Hills, Nowell and O'Connor (1988)] modelled fretting fatigue cracks as a crack edge of a half plane, perpendicular to the surface, and found that cracks are generally closed and most likely to propagate in mode II.

In contrast, other researchers insert an inclined crack at a location calculated based on the stresses at contact and then assess its propagation. Faanes [Faanes (1995)] was one the first researchers to consider an initial inclined crack and attempted to compute the error of considering it in a vertical direction instead of oblique one. Based on his findings, in most of the cases, the assumption of pure mode I propagation is valid. However, under conditions of high contact pressure, where crack closure may happen, the assumption of pure mode I may lead to very conservative life estimates.

The orientation of the initial crack may be based on experimental data. However, many methods for predicting the orientation angle of this initial crack have been proposed. The Critical Plane (CP) approaches are used for this purpose. These may be classified as stress based, strain based, and strain energy based [Bhatti and Abdel Wahab (2018)]. Some stress based parameters are the Findley Parameter (FP), the McDiarmid (MD) parameter, and the Shear Stress Range (SSR) parameter. Strain based examples are the Fatemi-Socie (FS) parameter and the Brown-Miller (BM) parameter. Lastly, the Smith-

Watson-Topper (SWT) and Lui parameters are strain energy based. One of the most used is the SWT.

The FP and MD parameters are similar damage parameters that can be applied for High Cycle Fatigue (HCF). They are based on the fact that crack initiation is influenced by the maximum shear stress range and also by the maximum normal stress acting on the plane of maximum shear stress range. The FP may be more appropriate when shear is the dominant failure mode and when initiation and propagation directions are the same. The MD parameter may be applied for cracks growing parallel or into the surface. The SSR is a similar parameter that is also based on the shear stress range. However, Namjoshi et al. [Namjoshi, Mall, Jain et al. (2002)] found that the SSR parameter, as well as the SWT parameter, but opposite to FP, are dependent of pad geometry. To overcome this problem, the Modified Shear Stress Range (MSSR) was proposed; this introduces a normal stress term. In general, the stress-based parameters are more appropriate when shear is the dominant failure mode and for HCF. Also, shear based parameters are the ones to select to determine crack initiation orientation. Regarding the strain based parameters, the BM parameter is similar to FP and MD, but it is based on strain rather than on stress. The FS parameter is a modification of the BM parameter to incorporate the effects of non-proportional loads. It replaces the BM normal strain term by a normal stress term, and it is appropriate for shear mode failure. Strain based parameters may be more suitable when plasticity effects are of greater importance, e.g., for LCF and higher load amplitudes. The SWT (strain energy based) is one of the most used, as mentioned before, and may be employed for Low Cycle Fatigue (LCF) and HCF when mode I is the dominant failure mode. It considers non-proportional and mean stress effects. The SWT parameter is defined as the product of the maximum tensile stress and the strain range. Finally, Lui parameters show good prediction capability and are for shear dominated failure and the tensile dominated failure. Strain energy based parameters are a good choice for flat pads and pads with small radii; in these cases higher stress gradients are exhibited, and cyclic plastic deformations play an important role [Bhatti and Abdel Wahab (2018)].

According to the review of Bhatti et al. [Bhatti and Abdel Wahab (2018)], predicted initiation angles (by CP approaches) are commonly positive and in the range [25°, 50°], but negative values have been also predicted, i.e., the crack would grow outside the contact region (to the left in Fig. 9). For instance, several authors have found numerically that the crack would grow outside the contact region [Lykins, Mall and Jain (2000); Naboulsi and Mall (2003); Li, Zuo and Qin (2015); Bhatti and Abdel Wahab (2017a); Pereira, Bhatti and Abdel Wahab (2018)].

When computing the CP damage parameter for determining crack initial location and orientation, most works use the point method [Szolwinski and Farris (1998); Lykins, Mall and Jain (2001a); Namjoshi, Mall, Jain et al. (2002); Araújo and Nowell (2002); Navarro and Domínguez (2004); Li, Zuo and Qin (2015); Bhatti and Abdel Wahab (2017b)]. That is to say, the surface point that has the maximum value of the damage parameter is where the crack will nucleate, and the orientation of that initial crack would be the one for which that maximum value was obtained. This is reasonable, but this approach may not be appropriate when there are high stress gradients, as stresses may be overestimated in the models.

Consequently, when there are very high stress gradients or stress singularity, when the pad has sharp corners, stress averaging methods may be required. When using these averaging methods, subsurface stresses are also taken into account. This may be achieved by the line method, in which the damage parameter is calculated at some points along radial lines, or the volume (area) method, in which the parameter is determined at certain points within a volume. In both cases, the damage parameter is calculated as the average of the values of the points considered in the line or the area. The volume method may be more appropriate when the critical region is small, as the line method would only consider one or two points. Consequently, the volume method has been used by many authors [Araújo and Nowell (2002); Naboulsi and Mall (2003); Navarro and Domínguez (2004); Proudhon, Fouvry and Buffière (2005); Hojjati-Talemi, Abdel Wahab, Giner et al. (2013); Hojjati-Talemi and Abdel Wahab (2013); Hojjati-Talemi, Abdel Wahab, De Pauw et al. (2014); Bhatti and Abdel Wahab (2018); Bhatti, Pereira and Abdel Wahab (2018)]. Nevertheless, Bhatti et al. [Bhatti, Pereira and Abdel Wahab (2019)] recently proposed a modified averaging method (named quadrant method). In this method, the critical region is divided into two zones (named left and right quadrants), and the damage parameter is calculated in each quadrant. The quadrant that has the greater value of the damage parameter corresponds to the zone in which, more probably, the crack will grow. Their results suggest that the proposed approach produces more appropriate estimations of crack direction than volume averaging and point methods.

3.4 Crack initiation length

Fracture mechanics approach for propagation depends upon the definition of a "crack initiation length", which separates the initiation and propagation phases. Many works in the literature have considered that this length is the minimum one that could be used in fracture mechanics [Madge, Leen and Shipway (2008); Cardoso, Araújo, Ferreira et al. (2016)]. It is determined by El-Haddad parameter [El Haddad, Smith and Topper (1979)]:

$$a_0 = \frac{1}{\pi}\left(\frac{\Delta K_{th}}{\sigma_A}\right)^2 \tag{15}$$

where σ_A is the material's fatigue limit and ΔK_{th} is the minimum Stress Intensity Factor (SIF) threshold that produces crack propagation.

This size is commonly maintained constant, and, therefore, the influence of contact size and stress gradients is disregarded. Also, calculating the initial length with Eq. (15) is arbitrary from a phenomenological point of view [Navarro, García and Domínguez (2003)].

In addition, Noraphaiphipaksa et al. [Noraphaiphipaksa, Kanchanomai and Mutoh (2013)] determined, through a sensitivity study, that selecting an initial crack length equal to half the value obtained by Eq. (15) provides a more suitable value, when comparing the obtained numerical results with experimental data. However, both methods are somewhat arbitrary, because they are not based on the phenomena involved, but rather on the limitations of the approach used (fracture mechanics) or limited experimental data.

In contrast, Navarro et al. [Navarro, García and Domínguez (2003)] proposed an approach to determine a non-arbitrary crack nucleation length (variable initiation length method).

The fatigue crack propagation rate da/dN, where a is crack length and N is number of cycles, is calculated by initiation mechanisms and propagation mechanisms. The crack length for which both values of da/dN are equal is the crack initiation length. Thus, when a is shorter than this length, da/dN for initiation mechanisms is greater than its counterpart for propagation laws, and initiation mechanisms predominate. The opposite is the case when a is longer than the initiation length. This seems reasonable, but it corresponds to a conservative approach; therefore, fatigue lives might be underestimated.

Also, Gandiolle et al. [Gandiolle and Fouvry (2016)] calculated an optimum initiation length that may be used in conjunction with the Theory of Critical Distance (TCD). The optimum length is the one related to the minimum prediction error of cracking risk.

However, many researchers have selected arbitrarily the initiation crack length [Llavori, Zabala, Urchegui et al. (2019)]. Crack initiation length may be related to microscopic material features. For example, as stated by Marco et al. [Marco, Infante-García, Díaz-Álvarez et al. (2019)], the length of a propagation stage crack is at least several times higher than the characteristic grain size. Also, it has been based on non-destructive testing resolution [Lykins, Mall and Jain (2001b)]. Commonly, this size is taken between 10 μm and 1 mm, but mostly up to 100 μm [Bhatti and Abdel Wahab (2018)].

As there is not an agreement of crack initial size, the calculations for initiation and propagation lifetimes would vary depending on how the initial length is selected. Therefore, further research is needed regarding the definition of the initial crack for crack propagation stage.

3.5 Stress averaging

Depending on the methodologies employed to study fretting fatigue crack initiation, stress averaging may be necessary when there are high stress gradients or singularities. For calculating the value of a damage parameter, usually, the point, the line, and the volume (area) methods are used, as already discussed in Section 3.3. Of these three, the line and volume methods are averaging methods.

Some authors have employed or analysed the use of these methods. For instance, Redford et al. [Redford, Gueguin, Nguyen et al. (2019)] used volume averaging when computing stresses through FEM for predicting fretting fatigue crack nucleation in strands of steel-reinforced aluminium conductors for overhead power lines. They used the multiaxial HCF CP initiation criterion of the maximum shear stress. They obtained the stresses for the stable state through the stationary incremental method [Dang Van and Maitournam (1993)]; thus, plastic deformation was considered. The stationary method reduces the computational time, when the stabilised state is reached, usually in about 20 cycles. The authors argued that there is autonomy in the selection of the averaging box size, within nonlocal methods for considering stress gradients, as there is not a consensus for its selection for fretting fatigue. However, the calculated damage varied with the averaging box size (more damage for smaller volumes), and a suitable volume averaging size would have to be determined experimentally.

Also, Bhatti et al. [Bhatti, Pereira and Abdel Wahab (2019)] numerically dealt with stress averaging and the suitability of a proposed modified averaging method (named quadrant

method, as explained in Section 3.3) on crack initiation orientation and lifetime. This method is compared with conventional point and volume averaging methods. They used the Fatemi Socie (FS) and McDiarmid (MD) multiaxial CP parameters. The materials and configurations studied are aluminium alloys 2024-T351 and 7075-T6 and cylindrical and flat pads, respectively. The results suggest that the proposed approach produces more appropriate estimations of crack direction than volume averaging and point methods. Also, regarding the stress averaging critical radius, it was concluded that it should be chosen based on the decay rate of the damage parameter and the degree of stress gradient.

As a conclusion, stress averaging methods are important, as they tend to lead to more accurate estimations of crack initiation location, orientation, and lives. They are particularly necessary for flat-to-flat contacts and when the radii of the cylindrical indenter are small, as stress gradients are higher in these cases. However, more research is needed so that suitable critical radii for averaging may be determined, preferably from a phenomenological point of view or at least from sufficient experimental information. According to Bhatti et al. [Bhatti, Pereira and Abdel Wahab (2019)], this critical length depends on several factors such as geometry, size of contact, values of the loads, material, and damage model, and it is generally in the range [5, 80] μm. At present, this critical radius is often determined from experimental fitting or is commonly taking equal to El-Haddad parameter (Eq. (15)).

3.6 Out of phase loading

The majority of works on fretting fatigue tackle the case of constant normal force and in-phase loading [Bhatti, Pereira and Abdel Wahab (2018)]. However, there are cases in which this does not occur. For example, in aero-engine compressor blade-disk dovetail assemblies, a fluctuating speed produces variable centrifugal forces which in turn lead to variable normal contact pressures. Consequently, some researchers have studied out of phase loading, and here some works that have performed fretting fatigue initiation analyses for this case are reviewed.

For instance, Almajali [Almajali (2006)] investigated the influence of out-of-phase application of bulk and contact loads on fatigue behaviour of Ti-6Al-4V by means of experimental tests and FEM. Lifetimes, as well as crack nucleation location and direction, were calculated with accuracy using the Modified Shear Stress Range (MSSR) Critical Plane (CP) fatigue parameter. Also, as may be expected, experimental cracks consistently nucleated near the trailing edge. According to the results, lifetimes were nearly the same when the contact load was constant and when it varied in-phase, and lifetimes were higher for the out of phase loading than in-phase case. In contrast, Lee et al. [Lee and Mall (2006)], also using the MSSR parameter, found no significant influence of phase difference on lifetime.

Bhatti et al. [Bhatti, Pereira and Abdel Wahab (2018)] also studied out-of-phase loading, for fretting fatigue crack nucleation of Al 2024-T351 and Ti-6Al-4V. The purpose of the paper was to explore the effectiveness of CDM for loads under phase difference, including variable normal force. They also applied the CP approach and compared both methodologies with experimental data from the literature. They concluded that both methods provide suitable estimates of initiation site and lifetimes for phase difference of

0 (i.e., in-phase loading) and 90°. Nevertheless, CDM provides lifetime predictions that are in more agreement with experimental findings. Also, similar to Almajali [Almajali (2006)], the two methods showed that for a phase difference of 90°, the High Cycle Fatigue (HCF) lifetime is larger than that for in-phase loading. It was also found that when the axial and tangential loads are out of phase, nucleation may occur at whichever contact edge. In contrast, when the normal force is out of phase from the other loads, the nucleation site is exhibited at the trailing edge.

Similarly, Bhatti et al. [Bhatti and Abdel Wahab (2017b)] studied three phase difference angles: 0°, 90°, and 180°. The Smith-Watson-Topper (SWT) and Ruiz parameters were used. By applying both parameters and validating by means of experimental data, it was found that, for 0°, nucleation would occur at the trailing edge of contact, as expected, but, for 180°, it would occur at the leading edge. Also, as in Bhatti et al. [Bhatti, Pereira and Abdel Wahab (2018)], for 90°, damage would be exhibited at either contact edge.

4 Crack propagation

4.1 Crack face interaction

During the propagation phase of fretting fatigue, crack face interactions may be exhibited during a loading cycle. Therefore, frictional adhesion or slip may have to be modelled for the crack, in addition to the pad-specimen interaction. Furthermore, crack closure effects (induced by plasticity, corrosion, and surface roughness) may have to be taken into account. This further complicates the problem. As crack face contact can influence growth rate, it has a direct impact on the life predictions obtained by fracture mechanics [Giner, Sabsabi and Fuenmayor (2011)].

Dealing with fretting in steel samples, Noraphaiphipaksa et al. [Noraphaiphipaksa, Manonukul, Kanchanomai et al. (2014)] showed that fretting fatigue crack closure and opening behaviour may be significant. In a latter study, Noraphaiphipaksa et al. [Noraphaiphipaksa, Manonukul, Kanchanomai et al. (2016)] conducted experiments and FE simulations of flat-on-flat fretting fatigue configuration, aiming to evaluate the impact of crack closure behaviour under those conditions. Using strain gauge measurements near the crack mouth and the relationship between those measurements and the applied bulk stresses, they were able to determine the crack opening load. They detected that crack opening may take place under alternating compressive bulk load, because of the effect of contact stresses on the behaviour of the crack. This idea was further supported by their numerical analysis. They determined numerically the crack opening ratio α based on the stresses at crack mouth at maximum load σ_{max} and at opening load σ_{OP}:

$$\alpha = \frac{\sigma_{max} - \sigma_{OP}}{\sigma_{max}} \tag{16}$$

The crack opening load was numerically determined as the loading that makes zero the crack surface normal stress (at a distance of 10 μm of the mouth of the crack). In their study, they incorporated the crack opening and closure effect through a maximum effective range of SIF $\Delta K_{(max,eff)}$ given by:

$$\Delta K_{(max,eff)} = \alpha \, K_{max} \tag{17}$$

where K_{max} is the maximum SIF obtained by contour integral at the condition of maximum load. This effective stress was later used in combination with a fatigue crack growth law to predict lives under fretting conditions, and the results using $\Delta K_{(max,eff)}$ produced estimates in better agreement than using the traditional K_{max}.

Recently, Noraphaiphipaksa et al. [Noraphaiphipaksa, Manonukul and Kanchanomai (2017)] used the above methodology to study the impact of different pad geometries (flat and cylindrical with two different radii) on life estimates, incorporating the phenomenon of crack opening and closure (considering frictionless contact between crack faces) and its impact on fatigue crack growth. Their predictions of propagation path were in agreement with experimental observations. However, shorter lives were obtained for cylindrical contact when compared with flat pad. Regarding total life estimates, they agreed with experimental observations, being slightly smaller. The authors argued that this was because they neglected plasticity-induced crack closure phenomena.

In addition, when modelling fretting fatigue through X-FEM, difficulties have surged, as crack faces are not physically modelled as in the standard FEM. Consequently, various methods for modelling crack face contact through X-FEM have been proposed [Giner, Sabsabi and Fuenmayor (2011)]. For example, Dolbow et al. [Dolbow, Moës and Belytschko (2001)] and Ribeaucourt et al. [Ribeaucourt, Baietto-Dubourg and Gravouil (2007)] presented X-FEM models that account for Coulomb friction crack face contact. The solution was obtained through the LATIN method. However, only the latter work dealt with fretting fatigue. Similarly, Pierres et al. [Pierres, Baietto, Gravouil et al. (2010)] and Baietto et al. [Baietto, Pierres and Gravouil (2010)] used linear interface elements with Gauss points, along the crack faces, for dealing with crack face frictional contact. In these works, Coulomb friction was also used.

Lastly, Giner et al. [Giner, Sabsabi and Fuenmayor (2011)] proposed two different methods for dealing with crack face interaction. In the first one (the point constraint approach), they used 2-degree-of-freedom one-dimensional truss elements of negligible stiffness (T2D2 elements in ABAQUS). These elements connect two nodes on the two crack faces and avoid crack face interpenetration at the location of the nodes. The second method is based on the mortar method. It is a segment-to-segment method, along the faces of the cracks, where the contact conditions have to be satisfied. Thus, crack face interference is prevented through the faces. According to the authors, the constraint conditions are satisfied with much higher accuracy than with the truss elements, and no extra elements or nodes are required.

4.2 Orientation criteria for crack propagation stage

4.2.1 Overview

One important point of modelling the fretting crack propagation stage is the determination of crack growth direction. However, due to the mixed-mode and non-proportional loading characteristics of fretting, this is not an easy task. For example, as stated by Lamacq et al. [Lamacq, Baïetto-dubourg and Vincent (1996)], depending on the loading conditions, either mode I or mode II may be dominant; also, mode II, under a

spherical contact situation, is mainly due to the interaction between the two cracks that appear symmetrically in the problem.

According to a study of Marco et al. [Marco, Infante-García, Díaz-Álvarez et al. (2019)], the most relevant factors that influence the direction of a stage II crack in a complete contact fretting fatigue case are the relative Young's moduli of specimen and pad, the COF between them, and the pad width. In contrast, the normal and cyclic bulk forces do not have a significant effect on crack propagation direction. For this study, they applied the minimum shear stress range criterion (Section 4.2.7) and assumed an initial crack perpendicular to the contact surface. The results (crack paths) were validated through experimental data.

In order to determine appropriate crack orientations, many crack growth direction criteria have been proposed and utilised for the case of proportional mixed-mode fatigue. An outline on this may be obtained in the literature [Rozumek and Macha (2009)]. These classical LEFM orientation criteria for proportional loading estimate crack propagation orientations with suitable accuracy [Pereira and Abdel Wahab (2017)]. Some of the criteria are the Maximum Tangential Stress (MTS) [Erdogan and Sih (1963)], the Maximum Energy Release Rate (MEER) [Nuismer (1975)], the minimum strain energy density factor *S* [Sih (1974)], and the "local symmetry" [Cotterell and Rice (1980)] criteria.

Nevertheless, these classical criteria may not be suitable for the case of non-proportional loading (e.g., for the fretting case), and other criteria have been proposed for this case. There are many works related to crack propagation orientation; however, we concentrate on some of the most pertinent to fretting fatigue. Fig. 10 presents common orientation criteria that will be described in this section. Firstly, we describe the criteria for proportional loading. Secondly, the criteria that have been proposed for non-proportional loading and, therefore, that are more appropriate for estimating fretting fatigue crack propagation orientation are presented.

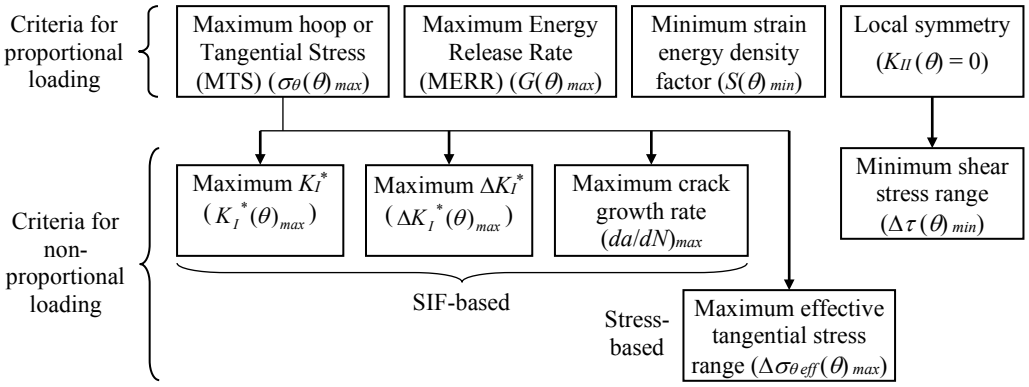

Figure 10: Orientation criteria for crack propagation

It has to be mentioned here that, for mixed-mode and non-proportional loading, there is not yet a consensus regarding the appropriate criteria for crack propagation orientation. Therefore, more research is necessary to increase the understanding of the phenomena involved in crack growth under this loading conditions and to understand which orientation

criteria may be suitable for different geometries, loading conditions, and materials.

4.2.2 Maximum Tangential Stress (MTS)

According to the Maximum Tangential Stress (MTS) criterion, originally proposed by Erdogan et al. [Erdogan and Sih (1963)], propagation occurs in the radial direction θ_P of largest tensile stress. In other words, the crack grows in the direction in which the tangential or hoop stress σ_θ is maximum. Therefore, according to this criterion, the crack will grow under the opening mode (mode I), which is a suitable assumption for brittle materials. According to Erdogan et al. [Erdogan and Sih (1963)], the fracture mode for ideal brittle materials seems to be always mode I, but this is not always the case for materials that exhibit a plastic zone around the crack front.

The hoop stress is a function of the SIFs for mode I and II, K_I and K_{II}, respectively:

$$\sigma_\theta = \frac{1}{\sqrt{2\pi\, r}} \cos\frac{\theta}{2}\left[K_I \cos^2\frac{\theta}{2} - \frac{3}{2} K_{II} \sin\theta \right] \tag{18}$$

where r and θ are the cylindrical coordinates of the point of interest, as shown in Fig. 11.

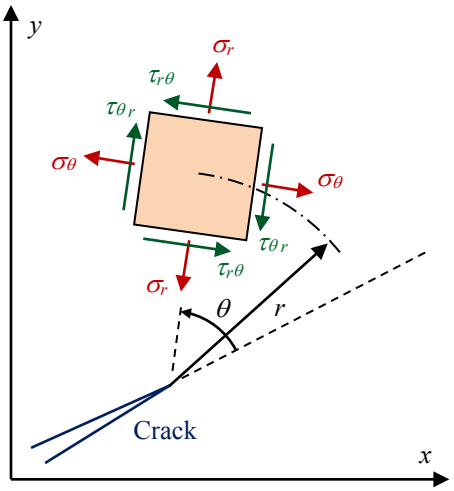

Figure 11: Stresses at a point in polar coordinates

Imposing the conditions $\frac{\partial \sigma_\theta}{\partial \theta} = 0$ and $\frac{\partial^2 \sigma_\theta}{\partial \theta^2} < 0$, the direction of propagation θ_P can be obtained as a function of K_I and K_{II}:

$$\theta_P = \cos^{-1}\left(\frac{3K_{II}^{\,2} + \sqrt{K_I^{\,4} + 8K_I^{\,2}K_{II}^{\,2}}}{K_I^{\,2} + 9K_{II}^{\,2}} \right) \tag{19}$$

4.2.3 Maximum Energy Release Rate (MERR)

The Maximum Energy Release Rate (MERR) criterion, proposed by Palaniswamy et al. [Palaniswamy and Knauss (1978)] and Hussain et al. [Hussain, Pu and Underwood

(1974)] states that the crack propagates with an orientation θ_P that maximises the energy release rate $G(\theta)$. This seems reasonable, as G is the driving force for fracture. For proportional loading, MERR results are the same as the MTS counterparts [Giner, Sabsabi, Ródenas et al. (2014)]. For the case of mixed mode conditions and co-planar crack propagation, $G(\theta)$ may be given by

$$G(\theta)=\frac{1}{E'}\left(K_I^{*2}(\theta)+K_{II}^{*2}(\theta)\right) \tag{20}$$

where $E'=E$ for plane stress and $E'=\frac{E}{1-\nu^2}$ for plane strain conditions; $K_I^*(\theta)$ and $K_{II}^*(\theta)$ are the SIFs for the new crack front at a branched (kink) small crack from the initial one (Fig. 12).

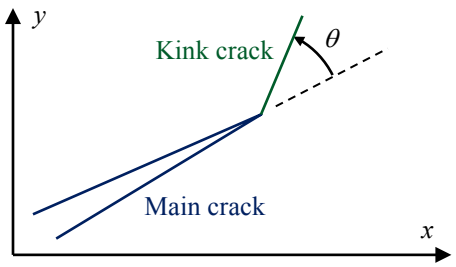

Figure 12: Crack kinking

The SIFs for the kink crack may be obtained by Ribeaucourt et al. [Ribeaucourt, Baietto-Dubourg and Gravouil (2007)]:

$$K_I^*(\theta)=C_{11}(\theta)K_I+C_{12}(\theta)K_{II} \quad \text{and} \quad K_{II}^*(\theta)=C_{21}(\theta)K_I+C_{22}(\theta)K_{II} \tag{21}$$

where the parameters C_{ii} may be obtained from the literature [Martínez, Vanegas-Useche and Abdel Wahab (2017); Ribeaucourt, Baietto-Dubourg and Gravouil (2007)].

According to MERR, crack growth direction may be estimated by:

$$\left.\frac{\partial G(\theta)}{\partial\theta}\right|_{\theta=\theta_P}=0 \quad \text{and} \quad \left.\frac{\partial^2 G(\theta)}{\partial\theta^2}\right|_{\theta=\theta_P}\le 0 \tag{22}$$

4.2.4 Minimum strain energy criterion

According to this criterion, the crack will grow with an orientation θ_C for which the function of the strain energy density $S(\theta)$ is minimised. The factor S "represents the strength of the elastic energy field in the vicinity of the crack tip" and is given by Sih [Sih (1974)]

$$U=\frac{1}{2}\sigma_{ij}\varepsilon_{ij}=\frac{S(\theta)}{r}=\frac{1}{r}\left(a_{11}K_I^2+2a_{12}K_IK_{II}+a_{22}K_{II}^2\right) \tag{23}$$

where U is the singular strain energy density related to the stresses near the tip of the crack. The coefficients in Eq. (23) are given by

$$a_{11} = [(1+\cos\theta)(\kappa-\cos\theta)]/(16\pi\, G_s)$$
$$a_{12} = \sin\theta\,[2\cos\theta-\kappa+1]/(16\pi\, G_s) \quad (24)$$
$$a_{22} = [(\kappa+1)(1-\cos\theta)+(1+\cos\theta)(3\cos\theta-1)]/(16\pi\, G_s)$$

where κ=3-4ν for plane strain and κ=(3-ν)/(1+ν) for plane stress, and G_s is the shear modulus.

4.2.5 Criterion of local symmetry

The "local symmetry" criterion see [Goldstein and Salganik (1974); Cotterell and Rice (1980)] assumes that the crack propagation orientation is the one for which K_{II}=0. That is, it is assumed that the crack grows under pure mode I; therefore, this criterion would be appropriate for brittle materials. The calculation of K_{II} has to take into account crack face friction for the time the crack is closed. This may be difficult and lead to inaccuracies when utilising contour and domain integrals [Giner, Sabsabi, Ródenas et al. (2014)].

4.2.6 Extensions of the MTS criterion

As mentioned before, the problems of fretting fatigue involve non-proportional loading, for which those criteria do not apply. For instance, various researchers tried to make use of traditional LEFM orientation criteria using numerical models, but their fretting fatigue path predictions were not in agreement with experimental observations [Hojjati-Talemi, Abdel Wahab, De Pauw et al. (2014); Giner, Sabsabi, Ródenas et al. (2014); Giner, Sukumar, Denia et al. (2008)].

Hourlier et al. [Hourlier, D'Hondt, Truchon et al. (1985)] proposed three extensions of the classical MTS criterion for non-proportional loads, based on SIFs. They are based on the K_I^* values, along the fatigue cycle. K_I^* and K_{II}^* are the mode I and mode II, respectively, SIFs of a kink crack, as explained before (see Fig. 12 and Eq. (21)). The three extensions (which are based on the CP concept) are described as follows:

- The first extension proposes that crack grows with an orientation that maximises the mode I SIF for a branched crack, considering the entire load cycle. In other words, crack grows with the orientation in which $K_I^*(\theta)$ is maximum ($K_I^*(\theta)_{max}$). Under proportional loading, this criterion is the same as the classical MTS.
- The second extension considers the orientation in which the amplitude of $K_I^*(\theta)$ is maximised during the cycle ($\Delta K_I^*(\theta)_{max}$).
- A major drawback of both extensions described above is that they do not consider mean stress effects. In order to solve that, the third extension proposes that the orientation θ for crack growth is which maximises crack growth rate, i.e., $(da/dN)_{max}$.

Instead of dealing with SIFs, another approach ("fourth extension") is to define an orientation criteria based on stresses at crack tip. Dubourg et al. [Dubourg and Lamacq (2000)] suggested that the crack propagates in the direction that, during the loading cycle, has the maximum effective amplitude of hoop stress at the front of the crack ($\Delta\sigma_{\theta,eff}(\theta)_{max}$). They also applied the first and second extensions of the MTS criterion. Their predictions

were validated with experimental data from fretting wear tests conducted with pre-stressed specimen under spherical contact. The results of the $\Delta\sigma_{\theta,eff}(\theta)_{max}$ criterion and the second extension of the MTS were similar and agreed with experimental findings. In contrast, the results of the first extension did not. As a conclusion, their work pointed out the necessity to account for non-proportional loading while predicting propagation paths, as the path predictions were better estimated using a proper criterion. Also, their results highlight that it is more suitable to evaluate ranges ($\Delta K_I^*(\theta)_{max}$ o $\Delta\sigma_{\theta,eff}(\theta)_{max}$) than maximum values [Giner, Sabsabi, Ródenas et al. (2014)].

Noraphaiphipaksa et al. [Noraphaiphipaksa, Kanchanomai and Mutoh (2013); Noraphaiphipaksa, Manonukul, Kanchanomai et al. (2016)] used the orientation criteria proposed by Dubourg et al. [Dubourg and Lamacq (2000)]. In order to reduce the dependency of the results on the radius of the circle (with centre at the crack tip) in which the stress were extracted, they performed a sensitivity study considering different radii. They found that, for the case of flat pad and flat specimen in steel, the radius that provided better accuracy when comparing predicted paths with experimental data was equal to half of the critical shortest crack. In addition, the results improved when this critical smallest crack length was also used as the initial size for crack propagation and as the increment size of crack growth for each analysis step. They also studied the influence of stress amplitude on paths. For the same contact pressure, they concluded that higher stress amplitudes led to paths turning into perpendicular direction to bulk load in an earlier stage. Lives were calculated with good agreement with experimental data, but not very accurate estimates were obtained for cases with high stress amplitudes. In these cases, the predicted lives were greater than the measured lives. They justified the mismatch by the fact that the plasticity zone ahead of the crack tip was neglected in their simulations.

Baietto et al. [Baietto, Pierres, Gravouil et al. (2013)] developed a methodology based on the combination of experimental data and numerical modelling to predict crack initiation and propagation. Crack face contact and friction were considered in their numerical scheme [Baietto, Pierres and Gravouil (2010)]. They compared the extensions of the MTS criterion suggested by Hourlier et al. [Hourlier, D'Hondt, Truchon et al. (1985)] and predicted propagation behaviour for 2D and 3D cases. Their results showed that crack paths could be accurately estimated using either the second or the third extensions $\Delta K_I^*(\theta)_{max}$ or $(da/dN)_{max}$. Nevertheless, the first extension $K_I^*(\theta)_{max}$ failed to predict correct paths.

Recently, Pereira et al. [Pereira and Abdel Wahab (2017)] applied the $\Delta K_I^*(\theta)_{max}$ criterion for the cylinder-flat case, in order to ascertain whether improved predictions of crack growth could be obtained.

4.2.7 Minimum shear stress range criterion

This criterion was proposed recently. Giner et al. [Giner, Díaz-Álvarez, Marco et al. (2015); Giner, Sabsabi, Ródenas et al. (2014)] accounted for the effect of crack face interaction on the determination of fretting fatigue crack trajectory. They proposed an orientation criterion based on the minimisation of the amplitude of shear stress at the crack front along the stress range, accounting for non-proportional loading. This criterion of minimum shear stress

range ($\Delta\tau_{min}$) is an extension, for non-proportional loading, of the "local symmetry" criterion [Cotterell and Rice (1980)]. As always $\Delta\tau_{min}$ occurs on two mutually perpendicular planes, the direction for crack growth selected corresponds to the plane on which the range of the normal stress is larger. The reason for this is that on this plane the loss of frictional energy is smaller, and more energy would be available for crack growth.

Studying the configuration flat-on-flat, X-FEM predictions of crack propagation path by Giner et al. [Giner, Sabsabi, Ródenas et al. (2014)] agreed with experimental observations. Their numerical simulations indicated the necessity of considering crack face contact, especially under compressive bulk stresses, where mode II plays a significant role in the propagation. Similarly, Martínez et al. [Martínez, Vanegas-Useche and Abdel Wahab (2017)] implemented an X-FEM approach to model the propagation phase, incorporating the effects of crack face contact and using the minimum shear stress range criterion. By doing so, they estimated with acceptable accuracy the propagation path of a fretting fatigue crack in a Chinese railway shaft. However, the use of the $\Delta\tau_{min}$ criterion for a pad with cylindrical shape may produce inaccurate path estimates [Cardoso, Araújo, Ferreira et al. (2016)].

4.3 Fatigue crack propagation (FCP) rate

Prediction of crack propagation for mode I loading has been widely tackled by fracture mechanics, where crack growth is co-planar and normal to load direction [Plank and Kuhn (1999)]. Nevertheless, many mechanical systems withstand mixed-mode normal and shear loads, and appropriate crack growth criteria and rate laws that consider mixed-mode loading are necessary.

Most works in the literature utilise LEFM to model "long" crack growth phase under fretting conditions [Noraphaiphipaksa, Manonukul, Kanchanomai et al. (2016); Giner, Tur, Vercher et al. (2009); Araújo and Nowell (2002)]. For applying LEFM, the pre-existence of a crack of appropriate size is necessary, so that the assumption of small scale yielding applies.

As discussed by Hertzberg [Hertzberg (1996)], in the last century, several theoretical and empirical "laws" were proposed to model FCP rate. Many of them suggested that this rate depends on the applied stress and the crack length, and they mostly had a simple power relation form. However, it was in the 1960s, after a battle of FCP rate laws, that the role of the SIF as a controlling parameter of growth rate was completely appreciated. This could be realised, thanks to strategic experimental work performed by some researchers [Paris and Erdogan (1963); Paris and Sih (1965); Swanson, Cicci and Hoppe (1967)].

Consequently, most of crack propagation modelling using fracture mechanics has been based on Paris type fatigue crack growth laws. The relationship between the fatigue crack growth rate da/dN and the applied SIF range ΔK can be expressed, according to Paris law, as:

$$\frac{da}{dN} = C(\Delta K)^m \tag{25}$$

where C and m are experimentally determined material constants. However, they depend on the mean value of K, amongst other factors.

The propagation life N_p is then obtained by integrating the above equation:

$$N_p = \int_{a_i}^{a_f} \frac{da}{C(\Delta K)^m} \tag{26}$$

where a_i is the initial crack length and a_f is the critical length, which is the total crack length to failure, e.g., the one for which $K_{max}=K_c$, being K_c the fracture toughness.

Although fretting fatigue crack behaviour is influenced by mixed mode conditions, life predictions usually rely on fatigue crack propagation data for pure mode I [Szolwinski and Farris (1998); Araújo and Nowell (2002); Mutoh, Xu and Kondoh (2003); Navarro, García and Domínguez (2003); Navarro, Muñoz and Domínguez (2008); Giner, Navarro, Sabsabi et al. (2011)]. Usually, in Eq. (26), ΔK is taken for mode I:

$$\Delta K = \Delta K_{eff} = \begin{cases} K_{I,max}, & \text{if } K_{I,min} \le 0 \\ K_{I,max} - K_{I,min}, & \text{if } K_{I,min} > 0 \end{cases} \tag{27}$$

It is well known that the curve da/dN versus ΔK has a sigmoidal shape, in a logarithmic scale, and that Paris law (Eq. (25)) applies only in the central (linear) part. For "large" values of ΔK (when K_{max} is very close to K_c), local crack instabilities arise and increase in number [Hertzberg (1996)]. Thus, da/dN is greater than the value given by Eq. (25). In contrast, for "small" values of ΔK (when ΔK is very close to its threshold value for crack growth ΔK_{th}), FCP rate is smaller than the one given by Paris law (short crack behaviour). In view of this, modified Paris laws have been proposed, in order to consider aspects such as short crack behaviour and mode mixity, as discussed beneath.

Mutoh et al. [Mutoh and Xu (2003)] compared crack propagation curves for a fretting case and a pure mode I condition. They argued that the pure mode I growth curve is a satisfactory assumption except for the initial part of the propagation, where small crack behaviour and mean stress play a significant role. However, the general fracture path exhibits a clear region under mixed-mode conditions, which may influence the reliability of estimates, based on pure mode I opening. Therefore, some researchers have incorporated the effect of mixed-mode conditions in their estimates. For instance, Baietto et al. [Baietto, Pierres, Gravouil et al. (2013)] introduced the effect of loading mixity by replacing ΔK in Eq. (26) by an effective range of the stress intensity factor:

$$\Delta K = \Delta K_{eff} = \sqrt{\Delta K_I{}^2 + b\Delta K_{II}{}^2} \tag{28}$$

where b is function of the loading mixity and ΔK_I and ΔK_{II} are mode I and II respectively, SIF ranges, computed for a full fretting cycle analysed and obtained by

$$\Delta K_I = K_{I,max} - K_{I,min}, \quad \text{with} \quad K_I \ge 0, \quad \text{and} \quad \Delta K_{II} = K_{II,max} - K_{II,min} \tag{29}$$

where the subscripts *max* and *min* refer to the maximum and minimum SIFs for any given fretting cycle, respectively. Several researchers [Madge, Leen and Shipway (2008); Hojjati-Talemi, Abdel Wahab, De Pauw et al. (2014); Hojjati-Talemi (2014)] incorporated mixed-mode effects in their predictions assuming the variable b constant and equal to unity.

Navarro et al. [Navarro, García and Domínguez (2003)] studied the impact of introducing

crack growth threshold effect ΔK_{th} on life estimates. They considered the classical Paris law and two of its adjustments. The first one is performed by simply subtracting ΔK_{th} from ΔK:

$$\frac{da}{dN} = C\left(\Delta K - \Delta K_{th}\right)^m \tag{30}$$

and the second one is:

$$\frac{da}{dN} = C\left(\Delta K^m - \Delta K_{th}{}^m\right) \tag{31}$$

Their results showed that, for tests that failed, the Paris law gives reasonable estimates, even though it neglects the threshold effect. They also indicated the necessity of including short crack effects in the estimates.

Additionally, short cracks may grow under ΔK values lower than the threshold ΔK_{th} (which is meant for long cracks). To take this into account, several researchers used an approximated form of the SIF, considering that short cracks may grow faster than long cracks under certain circumstances [Navarro, García and Domínguez (2003); Madge, Leen and Shipway (2008)]. In this methodology, growth of a crack of length (a+a_0), where a_0 is El Haddad parameter (Eq. (15)), is used to describe the growth of a short crack of length a. Under this assumption, the effective SIF range adjusted for short crack growth $\Delta K_{eff,short}$ is approximated by

$$\Delta K = \Delta K_{eff,short} = \Delta K_{eff}\sqrt{\frac{a+a_o}{a}} \tag{32}$$

Nevertheless, Muñoz et al. [Muñoz, Navarro and Domínguez (2007)] stated that they have observed that this $\Delta K_{eff,short}$ approach leads to very high predictions of crack growth rates for short cracks. Therefore, they proposed to account for short crack behaviour by one of the following approaches. In the first one, a corrected SIF threshold range may be determined as a function of crack length:

$$\Delta K_{th,corr}(a) = \Delta K_{th}\sqrt{\frac{a}{a+a_o}} \tag{33}$$

where ΔK_{th} is the (long crack) SIF threshold range and a_0 is El Haddad parameter (Eq. (15)). The crack growth rate is, therefore, given by

$$\frac{da}{dN} = C\left(\Delta K^m - \left(\Delta K_{th}\sqrt{\frac{a}{a+a_0}}\right)^m\right) \tag{34}$$

where C and m are the Paris constants mentioned in Eq. (25).

In the second approach, $\Delta K_{th-corr}(a)$ is calculated by a more general equation obtained by Vallellano et al. [Vallellano, Domínguez and Navarro (2003)]:

$$\Delta K_{th,corr} = \Delta K_{th}\left(\frac{a^f}{a^f + {a_0}^f - {l_0}^f}\right)^{1/(2f)} \tag{35}$$

where a is length of the crack, f is an experimentally obtained parameter, and l_0 is the typical distance between the contact surface and the nearest micro-barrier (e.g., the nearest grain boundary). From Eq. (35), da/dN is given by

$$\frac{da}{dN} = C\left(\Delta K^m - \left(\Delta K_{th}\left(\frac{a^f}{a^f + {a_0}^f - {l_0}^f}\right)^{1/(2f)}\right)^m\right) \tag{36}$$

The previous Paris like laws (Eqs. (25), (30), (31), (34) and (36)) suggest that the FCP rate depends on the amplitude of the SIF (and on the stress amplitude) but not on the mean value of the SIF (and the mean stress). However, the mean SIF K_m, or the mean stress σ_m, affects the FCP rate, particularly for high ΔK values [Hertzberg (1996)]. Characterising the mean load level by the SIF ratio R_S=K_{min}/K_{max}, a relationship that takes into account mean stress effects was proposed by Forman et al. [Forman, Kearney and Engle (1967)]:

$$\frac{da}{dN} = \frac{C_m \Delta K^n}{(1 - R_S)K_c - \Delta K} \tag{37}$$

where C_m and n are empirical material constants.

The total fatigue life of a component is comprised of the initiation life (stage I) and the propagation life (stage II). This section concentrated on the LEFM approach for stage II crack growth, because, as mentioned before, a review on fretting fatigue crack initiation (stage I) is available in the literature [Bhatti and Abdel Wahab (2018)]. However, there have been some efforts to combine both phases in life predictions [Hojjati-Talemi (2014); Navarro, García and Domínguez (2003); Giner, Navarro, Sabsabi et al. (2011); Hojjati-Talemi, Abdel Wahab, De Pauw et al. (2014)].

Navarro et al. [Navarro, García and Domínguez (2003)] developed a procedure to combine initiation and propagation lives in order to obtain total failure life. Initiation life was obtained considering McDiarmid multiaxial fatigue criterion, and propagation life was estimated through Paris law with SIFs computed via analytical expressions. The results were in agreement with experimental data with reasonable accuracy. A similar approach was used by Giner et al. [Giner, Navarro, Sabsabi et al. (2011)]. They compared the impact of computing SIFs via X-FEM and via analytical expressions. Their life estimates were, for the majority of tested cases, in agreement with experimental data. They argued that the three cases with estimated lives much smaller than experimental ones were the cases with smallest pad radii, which causes a smaller contact region and concentrates the stresses in a smaller zone. This leads to greater initiation life that is not captured by their model. Hojjati-Talemi [Hojjati-Talemi (2014)] computed initiation life using CDM and estimated propagation lives using LEFM and a Paris law. Their results showed that initiation and propagation lives were a considerable percentage of total failure lifetime, showing the necessity of accurately modelling both phases. Regarding to

lifetime estimates, they were in good agreement with experimental data. Finally, Cyclic Cohesive Zone Model (CCZM), which uses a damage evolution law, has been proposed recently to estimate total fatigue life in a unified manner. The reader is referred to Pereira et al. [Pereira and Abdel Wahab (2020)] and Section 5.1 for more details.

5 Additional aspects

This section complements the review presented in the previous sections. It is focused mainly on the discussion of other aspects related to recent research on fretting fatigue FE modelling.

5.1 Cohesive zone model

LEFM applies under the assumption of small scale yielding. Thus, when the stresses generated in fretting fatigue are high, such that this assumption does not apply, other theories may be needed. The Cohesive Zone Model (CZM) is an alternative methodology that models non-linearly the process zone near the crack front. This approach expresses the process of fracture and degradation in a narrow zone near the crack front or the zone where it would initiate, by means of a constitutive law that is function of the stresses and separations through the cohesive region. Its central characteristic is that there is no limitation regarding the plastic zone size around the crack front, as the stresses at this zone are bounded by the material cohesive strength. This monotonic CZM may be used to determine the location and orientation for crack initiation. However, it cannot model damage accumulation. Therefore, the Cyclic Cohesive Zone Model (CCZM) may be employed for calculating damage accumulation under cyclic loads. An important advantage of CCZM is that it may be applied to model, in a unified manner, the entire failure process, i.e., crack nucleation and crack propagation. However, CCZM does not account for plasticity effects [Pereira and Abdel Wahab (2020)].

A few authors have proposed to use CZM and CCZM for fretting fatigue. Kim et al. [Kim and Yoon (2014)] studied fretting fatigue through a 3D FE CCZM and experimental bending tests for flat-on-flat configuration, for both sharp and rounded edges. The material employed is the aluminium alloy 7050-T7451. They concluded that the use of CCZM is appropriate for modelling fretting fatigue. Zhang et al. [Zhang, Liu and Zuo (2015)] also used CCZM, through X-FEM, for studying the usefulness of residual compressive stresses for systems under fretting fatigue crack growth. The case investigated was cylinder-on-flat, with material Al 2024-T351. Results indicate that the residual stresses change crack path and improve both nucleation and propagation lifetimes, particularly for high residual stresses and low bulk loads. Zhang et al. [Zhang, Liu and Zuo (2016)] also applied X-FEM in conjunction with CCZM for fretting fatigue of Al2024-T351, but for studying the effect of tangential load. They found that the higher the tangential load, the lower the nucleation and propagation lives and the higher the fraction of nucleation life with respect to the total lifetime.

Similarly, Pereira et al. [Pereira, Bhatti and Abdel Wahab (2018)] investigated, through X-FEM, the use of the CZM for fretting fatigue crack nucleation site and direction. The CZM was used in conjunction with the nucleation criteria: maximum nominal stress and quadratic traction separation. They studied aluminium alloys and cylindrical and flat indenters. Their results indicate that the CZM predicts with accuracy crack initiation site and direction, using the quadratic traction separation criterion. The maximum nominal

stress criterion estimated accurately the location of the initial crack, but not its direction. Based on experimental data, as well as the application of CP methods (Fatemi-Socie (FS) and Findley (FP) parameters), they concluded that CZM may be utilised for crack nucleation modelling, as the local law describes more realistically the stresses near the crack front, avoiding the inherent singularity in LEFM.

More recently, Pereira et al. [Pereira and Abdel Wahab (2020)] employed an extrapolation methodology in conjunction with CCZM to predict fretting fatigue life. The purpose is to avoid cycle-by-cycle calculations that result in greater computational cost. The configuration studied is flat-to-flat. The X-FEM approach is used together with cohesive segments; in this manner, stress singularity near the crack front does not have to be modelled, and, thus, the common enrichment functions are avoided. The results were compared with experimental data and conventional approaches. They indicate that the estimates of the CCZM are in a narrower error band than those found through classical methods. They concluded that CCZM may provide accurate predictions and is a suitable alternative for estimating fretting fatigue lifetimes for the configuration studied.

It may be concluded that CCZM is a promising alternative to model crack growth (both initiation and propagation stages), and more research is necessary so that more successful fretting fatigue implementation cases are incorporated into the literature. A main drawback of CCZM is that is more computationally demanding than LEFM. Therefore, it may be mainly used when LEFM does not apply.

5.2 Wear

Fretting wear has also an influence on fretting fatigue, but most studies on this disregard this influence, as this may not be as significant when partial slip predominates. In fretting wear process, materials are removed at the surface between the two bodies in contact. Nonetheless, material removal due to wear has an effect on contact and subsurface stresses. In fact, depending on fretting conditions, wear may reduce or increase fatigue life, as discussed in the following paragraphs. In view of this, some authors have included wear effects into fretting fatigue modelling [Madge, Leen, Mccoll et al. (2007); Argatov, Gómez, Tato et al. (2011); Zhang, Lu, Gong et al. (2017); Zhang, Lu, Zou et al. (2018); Zeng, Zhang, Lu et al. (2019); Llavori, Zabala, Urchegui et al. (2019); Cardoso, Doca, Néron et al. (2019)].

For example, Argatov et al. [Argatov, Gómez, Tato et al. (2011)], studying wire ropes, indicated that wear scars may decrease their fatigue lifetime, as they act as stress raisers. Similarly, Zeng et al. [Zeng, Zhang, Lu et al. (2019)], investigating fretting fatigue initiation in a full-scale press-fitted shaft, indicated that a wear scar produces stress concentration that causes crack nucleation at the scar edge. Contrary to these works, longer lives may be estimated when modelling wear [Llavori, Zabala, Urchegui et al. (2019)], as imminent cracks may be removed by wear. However, the effect of wear may not be very significant [Cardoso, Doca, Néron et al. (2019)].

Llavori et al. [Llavori, Zabala, Urchegui et al. (2019)] presented an X-FEM coupled model for fretting wear and fretting fatigue initiation and propagation. A 2D cylindrical contact was studied. It combined the Archard wear model, SWT parameter for crack initiation, Miner-Palmgrem damage rule, and Paris law. An approach based on the

Theory of Critical Distance (TCD) was used to determine the location for analysis and the initial crack size. X-FEM was employed in conjunction with the Archard wear model for crack propagation prediction. The SIFs were computed through Giner et al. [Giner, Sukumar, Tarancon et al. (2009)] domain integral. Analytical methods and experimental results from the literature were used to validate the approach. According to their results, the relative slip diminishes with crack growth, because of reduced local stiffness. They indicated that the modelling of wear and fatigue simultaneously enables to account for the effect of crack growth on wear. Removal of material due to wear may delay the nucleation of cracks and, therefore, longer lives may be expected, as stated before.

Likewise, Cardoso et al. [Cardoso, Doca, Néron et al. (2019)] studied through FEM the effect of wear on fretting fatigue life estimations. For this purpose, the geometry was updated to account for the volume loss due to wear. To estimate life, the multiaxial fatigue criteria of SWT, Findley, and Modified Wöhler Curve Method (MWCM) were employed, in combination with TCD. The material investigated was Ti-6Al-4V alloy, and the configuration studied is cylinder-on-flat. Their results were compared to both results from modelling in which wear was not considered and experimental data from tests carried out under partial slip fretting. For the case studied, in which partial slip occurs, the results indicate that accounting for wear may marginally improve lifetime prediction accuracy, as less scatter was exhibited. Nevertheless, the increase in accuracy might not compensate for the higher computational cost.

Also, Zeng et al. [Zeng, Zhang, Lu et al. (2019)] considered the effect of wear in fretting fatigue initiation. They modelled a full-scale press-fitted steel shaft through a 3D FE model. The Fouvry wear model was used in conjunction with Ince et al. [Ince and Glinka (2011)] mean stress correction approach, which in turn combines the SWT and Morrow approaches. They indicated that, as mentioned before, cracks may initiate at wear scars and not necessarily at the contact edge. However, the main purpose of the study was to analyse the effect of a stress relief groove at the contact edge. Their results indicate that the larger the groove depth and the smaller the groove radius, the lower the wear rate and the higher the fatigue life.

These examples of modelling wear in fretting fatigue analyses indicate that results may be unpredictable, as in some cases longer lives are estimated when taking into account wear, and in other cases the opposite is the case. Therefore, additional research is needed to gain a clear understanding on the effect of wear: in which cases does wear increase fatigue life? When does it reduce life? In which cases is it necessary to model wear in fretting fatigue problems?

5.3 Heterogeneity

The vast majority of fretting fatigue modelling works assume that the material as homogeneous. However, most materials have micro-defects such as inclusions, pores, or voids [Deng, Bhatti, Yin et al. (2020)]. This is particularly the case of some manufacturing techniques such as additive manufacturing, 3D printing, welding, and casting. Heterogeneity is an important issue, as it affects stresses and strength and therefore could have an impact on lifetime and performance of a component. Consequently, a few authors have studied the effect of heterogeneity on fretting fatigue

[Zhang, McDowell and Neu (2009)].

Kumar et al. [Kumar, Biswas, Poh et al. (2017)] are the first to study numerically the effect of heterogeneity on the stress fields in fretting problems. They studied the cylindrical-on-flat configuration and introduced, in an orderly manner, circular voids throughout the specimen. The results indicate that indeed the introduction of voids affects stress distributions, particularly shear stresses. Also, peak stresses may shift from the contact surface to the surfaces of micro-voids, and peak shear stresses may be twice as high as those in a homogenous material.

Erena et al. [Erena, Vázquez, Navarro et al. (2018)] also investigated numerically the heterogeneous case and studied its effect on damage, through the SWT. They also studied a cylindrical-on-flat configuration but introduced one or three circular voids near the contact region. The results indicate that the damage parameter may diminish for some configurations of the voids; therefore, these may be used to improve fretting fatigue performance.

Similarly, Infante-García et al. [Infante-García, Giner, Miguélez et al. (2019)] studied the effect of heterogeneity on estimated fretting fatigue crack initiation life. Micro-voids of circular shape distributed in random and regular fashions were analysed. The configuration studied is cylinder-on-flat, and the material is Al 2024-T3. The McDiarmid (MD) and SWT parameters were used in conjunction with the maximum value and area approaches of the TCD, for predicting initiation life. Overall, the SWT predictions for crack initiation had a tendency to be in more agreement than MD predictions. As a conclusion, their results suggest that the presence of micro-voids significantly affects estimated initiation lives. In fact, they suggested that cracks do not necessarily nucleate at the usual contact edge (for homogeneous materials) but may form at a micro-void close to it. This would produce a shorter life. Nevertheless, according to the numerical results, micro-voids may increase life by reducing the SIF at the contact edge.

Likewise, Deng et al. [Deng, Bhatti, Yin et al. (2018)] dealt with the effect of heterogeneity on the stresses for the cylinder-on-plane fretting fatigue case. However, they studied the influence of micro-inclusions of various properties, shapes, and sizes, distributed randomly. Also, their effects on bulk material properties were studied through the Representative Volume Element (RVE). The work focused on two typical inclusions in the 2024-T3 aluminium alloy. From the FE and RVE results, it is shown that inclusion volume fraction and properties significantly affect bulk material Young's modulus, whereas inclusion shapes and sizes have a minor impact on them. Regarding the impact of inclusions on stresses, the results indicate that the maximum tensile stress is not highly affected by the presence of inclusions, whereas maximum shear stresses may occur at various locations in the specimen. Therefore, cracks may nucleate at different sites. Finally, crack paths tend to be affected by the stresses exhibited near adjacent inclusions.

To conclude, regarding further work, as discussed by Infante-García et al. [Infante-García, Giner, Miguélez et al. (2019)], experimental fatigue data are available for "homogeneous" materials, and data for porous materials may differ. Therefore, more experimental data would be needed for porous materials, made, for example, by additive manufacturing, and for heterogeneous materials in general. Additionally, materials with pores of other shapes and 3D modelling may be performed in the future. Pores with surface roughness or deformed due to manufacturing could be studied [Erena, Vázquez,

Navarro et al. (2018)]. Furthermore, various configurations, geometries, and materials should be studied to gain a suitable understanding of the effect of heterogeneity on fretting fatigue.

5.4 Crystal orientation

Fretting fatigue behaviour of crystalline materials is affected by factors such as crystal orientation [Gao, Hu, Wen et al. (2014)], structure, and size. Indeed, the properties of polycrystalline materials are not isotropic. In addition, the behaviour of single-crystal components subjected to fretting may be affected by crystal orientation. In view of this, a few authors have studied these issues.

Arakere et al. [Arakere, Knudsen, Swanson et al. (2006)] studied 2D and 3D subsurface stresses and the influence of crystal orientation on stresses and fatigue behaviour in single-crystal Ni-based superalloy, through FE and analytical approaches. It is noted that despite the importance of Ni-based alloys for turbine blades, fretting data is scarce [Fleury, Paynter and Nowell (2014)]. They studied cylindrical and spherical configurations. The criterion of the maximum shear stress amplitude was used, as it provided less scatter when comparing results with experimental data. The specimen (single crystal) was modelled as an anisotropic material. However, in the study, a frictionless contact was assumed. They concluded that the analytical solution may be used effectively, with the advantage of reduced computational demands. Also, the subsurface stresses and fatigue lives vary significantly with crystal orientation.

Likewise, Fleury et al. [Fleury, Paynter and Nowell (2014)] studied the effect of crystal orientation of a single-crystal Ni-based alloy cylindrical pad, in contact with a polycrystalline specimen, on the contact stresses and contact size. They performed high temperature fretting fatigue tests and modelled the problem through analytical and FE models. For FEM, the method of CD and volume stress averaging were adopted, and anisotropic material properties were considered for the pad. The averaging radius was taken equal to El Haddad's parameter. According to their results, the effect of crystal orientation on COF and the stresses generated perpendicular to the 2D problem analysed should be accounted for in order to obtain more accurate trends. It is noted that the COF was assumed constant, despite the fact that it varies with crystal orientation.

Recently, Han et al. [Han, Qiu, He et al. (2018)] studied the influence of two crystal orientations on fretting fatigue crack nucleation. The material studied is also a nickel-based single crystal superalloy, and the configuration is cylinder-on-flat. This work focused particularly on microscopic and plastic deformation aspects, for which experimental work and 3D crystal plastic FE modelling were performed. According to the FE and experimental results, fretting fatigue crack initiation behaviour depends significantly on crystallographic slip of Ni-based single crystal. For the two crystal orientations, the cracks nucleated along the slip line direction. The authors concluded that the FE model is effective for estimating crack nucleation.

6 Final comments and conclusions

This article discussed various aspects related to fretting fatigue modelling. An outline of the basic analytical stress solutions for non-conforming cylindrical contact was presented.

They include the classical Hertzian solutions for pressure distribution for the case of contact subjected to normal load. Also, stress solutions for the case of application of normal and tangential loads and the case of combining both with bulk loading (present in fretting conditions) were provided. This paper also discussed aspects of crack initiation such as initiation location, orientation, and length. Then, we concentrated on the propagation stage, dealing with crack face interaction, orientation criteria for crack propagation, and crack growth rate. Finally, additional aspects of fretting fatigue modelling were reviewed and discussed.

Analytical solutions have normally the advantage to be less computational demanding than numerical methods. However, they are restrictive and have several idealistic assumptions. Therefore, fretting is commonly modelled through numerical approaches. FE methodologies are popular in fretting fatigue research, as they enable improved modelling of complex problems with fewer assumptions, when compared with analytical methods. Therefore, the FEM may be suited for real life problems. FE modelling or X-FEM modelling, which does not require remeshing as the crack grows, are commonly employed. Important aspects of using these techniques in fretting fatigue are the contact problem, complex stress fields (multiaxial, non-proportional loads varying with time and position), mesh sizes, crack initiation, and propagation criteria and laws. Contact modelling is required for both the indenter-specimen contact and crack face contact. Therefore, it should include crack opening and closure and suitable contact methods (penalty method, Lagrangian and augmented Lagrangian multipliers) and friction modelling. The main goal of a FE implementation is not only accuracy of predictions. Other factors, such as convergence, computing time, versatility, and ease of application may be considered.

It could be stated that fretting fatigue is an important phenomenon, as it may reduce the lifetime of components subjected to contact loads and small oscillatory sliding. It is usually characterised by partial slip conditions and multiaxial, non-proportional, and high-gradient stresses. Wear and corrosion may also play an important role in fretting fatigue. However, these are commonly neglected in fretting fatigue studies.

Some of the important factors that affect fretting fatigue are the COF, slip amplitude, and contact pressure. However, other factors also influence it, such as relative Young's moduli of specimen and pad and the pad width (for complete contact) [Marco, Infante-García, Díaz-Álvarez et al. (2019)]. Surface roughness has also an effect on fretting fatigue. On the one hand, it is argued that increasing surface roughness (e.g., by shot peening) may have a positive effect on fretting fatigue lives [Fu, Wei and Batchelor (2000)]. On the other hand, though very limited, numerical research on roughness effect on fretting fatigue indicates that higher roughness produces shorter lives. In fact, the effect of roughness depends on the way it is produced during manufacturing or surface treatments.

Fretting fatigue comprises two stages: crack nucleation and crack propagation. The nucleation stage is ruled by shear stresses, which form persistent slip bands. A leading crack tends to nucleate at the trailing edge of contact, as demonstrated both experimentally and by modelling. It tends to grow at an angle with respect to the direction normal to the surface inwards the contact zone, under the influence of contact stresses and mixed mode non-proportional loading. Then, it tends to orientate

perpendicular to the bulk stress and to propagate under mode I due to this stress.

Usually, modelling the initiation phase relies on methodologies based on physical observations, thermodynamics principles, or empirical laws. Typical approaches and damage parameters are CP, fretting specific parameters, stress invariants, and CDM. The CP approaches are very popular, as they may estimate initiation location and orientation. Several damage parameters have been proposed in the literature, which may be classified as stress based, strain based, and strain energy based. As mentioned before, a review on fretting fatigue crack nucleation is available [Bhatti and Abdel Wahab (2018)].

The propagation phase usually relies on LEFM and, particularly, on Paris like crack propagation laws. This is adequate for many cases, but when there are considerable plastic deformations, which may be produced by the large contact stresses, LEFM becomes inaccurate. Furthermore, Paris like propagation life laws usually rely on experimental data that may not be suitable for fretting fatigue, as it is characterised by mixed mode non-proportional loading. In contrast, CZM does not rely on the assumption of elastic stresses and is presented as a promising alternative [Pereira, Bhatti and Abdel Wahab (2018)].

For increasing fretting fatigue life, some palliatives may be employed. They may be divided into Erena et al. [Erena, Vázquez, Navarro et al. (2018)] palliatives that: change the geometry (e.g., by introducing micro-voids), modify the fields of contact stresses (e.g., by texturizing the surface or modifying its roughness), change the properties of the material at the surface (e.g., by coatings or heat treatments), and introduce compressive residual stresses.

This work has focused mainly on FE approaches to deal with fretting fatigue, as this is one of the most robust, developed, and widely used numerical method. Furthermore, there are many commercial software packages that are FE based. In FE analyses, the domain is divided into smaller elements, called finite elements, interconnected by nodes, and partial differential equations are solved for the meshed system. As the mesh has to conform to the boundaries, such as crack faces, this constitutes a drawback when modelling fracture growth.

However, there are other numerical techniques such as the Finite Difference Method (FDM) and Boundary Element Method (BEM). Thus, it is worth to mention here other numerical approaches for potential modelling of fretting fatigue problems. In FDM, differential equations are solved by approximating them with difference equations and are reduced to a system of algebraic equations that may be easy to solve. In the BEM, linear partial differential equations are solved, formulating them in boundary integral form.

As mentioned before, constructing a mesh might cause difficulties when modelling crack growth. Meshfree methods, which are based on the definition of nodal points (field nodes) only, are numerical techniques that have the purpose of avoiding certain problems that may arise in methods that need a mesh. For example, crack growth requires either remeshing in FEM or additional degrees of freedom in X-FEM. Also, when the object is subjected to large deformation, accuracy problems arise if the mesh elements become much distorted; the modelling of phase transformation is also difficult. A few of the meshfree methods that have been proposed are smooth particle hydrodynamics (the oldest meshfree method), reproducing kernel particle method, meshless local-Petrov Galerkin, isogeometric analysis, partition of unity, cracking particles method, Element-Free Galerkin Method (EFGM), collocation method. [Garg and Pant (2018)]

For example, the EFGM [Belytschko, Lu and Gu (1994)] is one of the meshfree methods with more contributions for fracture analysis. This method employed global weak form as its basic structure. Initially, the EFGM relied on the construction of shape functions through moving least square and Lagrange's multiplier for boundary condition enforcement; however, further improvements followed. The collocation method has a strong form description. It has the advantage that it is efficient in the construction of the system of equations, as no integration is needed. Also, shape functions are evaluated only at nodes (not at integration points). A drawback of the collocation method is that high-order derivatives have to be evaluated. Also, imposing natural boundary conditions and non-symmetric stiffness matrix presents difficulties. [Garg and Pant (2018)]

The cracking particle method, proposed by Rabczuk et al. [Rabczuk and Belytschko (2004)], is another meshfree method, for modelling arbitrarily oriented cracks. The growth of the crack is modelled by activating crack surfaces at individual particles, and there is no need to represent the topology of the crack faces. Further details on meshfree methods may be found in Garg et al. [Garg and Pant (2018)], who provided a review on this topic.

Another numerical approach that may be used for problems with material discontinuities, e.g., cracked bodies, is peridynamics. This is a recent formulation of continuum mechanics, proposed by Silling [Silling (2000)], that is based on equations in an integral form and with which there is no need to describe crack topology. Furthermore, no procedures such as smoothing the normal of the crack surfaces are need in peridynamics; these methods are usually employed in X-FEM, meshless methods, and other partition of unity approaches [Ren, Zhuang and Rabczuk (2017)]. An improvement of peridynamics is the dual-horizon peridynamics methodology, investigated, for example, by Ren et al. [Ren, Zhuang and Rabczuk (2017)]; dual-horizon is defined as "the dual term of the horizons centering at each material points". They developed a dual-horizon peridynamics approach that produces minimal spurious wave reflection and ghost forces when variable horizons are adopted.

Regarding remeshing, it could be mentioned that Areias et al. [Areias and Rabczuk (2017)] have proposed an edge-based, mesh adaptivity algorithm that avoids the variable mapping approach. The algorithm, for dividing tetrahedra, focuses on fracture and makes use of specific data such as damage variables or edge deformation. The classical screened Poisson equation is used to avoid ill-posed equilibrium problem when strain softening occurs. Also, a pre-ordering in new mid-edge nodes was introduced in order to circumvent non-tetrahedrizable prisms.

Finally, aspects in which there is a need of more research on fretting fatigue are a clear understanding of which damage parameters, orientation criteria, etc., are appropriate for different cases of crack nucleation and propagation. Also, the effect of micro-voids, crystal orientation, out of phase loading, and wear, among others, require more research.

Funding Statement: The first author would like to thank the financial support of the Research Foundation-Flanders (FWO), https://www.fwo.be/, FWO Lead Agency project: G018916N 'Multi-analysis of fretting fatigue using physical and virtual experiments'. The second author greatly acknowledges the financial support of the Faculty of

Engineering and Architecture of Ghent University, through the mobility fund of the Scientific Research Committee (CWO), https://www.ugent.be/ea/nl/onderzoek/cwo-steun.htm, and the Finite Element Modelling Research Group of Ghent University, https://www.finiteelementresearch.ugent.be/.

Conflicts of Interest: The authors declare that they have no conflicts of interest to report regarding the present study.

References

Almajali, M. (2006): *Effects of Phase Difference between Axial and Contact Loads on Fretting Fatigue Behavior of Titanium Alloy (Ph.D. Thesis)*. Air Force Institute of Technology, USA.

Arakere, N. K.; Knudsen, E.; Swanson, G. R.; Duke, G.; Ham-Battista, G. (2006): Subsurface stress fields in face-centered-cubic single-crystal anisotropic contacts. *Journal for Engineering for Gas Turbines and Power*, vol. 128, no. 4, pp. 879-888.

Araújo, J. A.; Nowell, D. (2002): The effect of rapidly varying contact stress fields on fretting fatigue. *International Journal of Fatigue*, vol. 24, no. 7, pp. 763-775.

Areias, P; Rabczuk, T. (2017): Steiner-point free edge cutting of tetrahedral meshes with applications in fracture. *Finite Elements in Analysis and Design*, vol. 132, pp. 27-41.

Argatov, I. I.; Gómez, X.; Tato, W.; Urchegui, M. A. (2011): Wear evolution in a stranded rope under cyclic bending: implications to fatigue life estimation. *Wear*, vol. 271, no. 11-12, pp. 2857-2867.

Baietto, M. C.; Pierres, E.; Gravouil, A. (2010): A multimodel X-FEM strategy dedicated to frictional crack growth under cyclic fretting fatigue loadings. *International Journal of Solids and Structures*, vol. 47, no. 10, pp. 1405-1423.

Baietto, M. C.; Pierres, E.; Gravouil, A.; Berthel, B.; Fouvry, S. et al. (2013): Fretting fatigue crack growth simulation based on a combined experimental and XFEM strategy. *International Journal of Fatigue*, vol. 47, pp. 31-43.

Belytschko, T.; Lu, Y.; Gu, L. (1994): Element free Galerkin methods. *International Journal for Numerical Methods in Engineering*, vol. 37, pp. 229-256.

Bhatti, N. A.; Abdel Wahab, M. (2017a): A numerical investigation on critical plane orientation and initiation lifetimes in fretting fatigue under out of phase loading conditions. *Tribology International*, vol. 115, pp. 307-318.

Bhatti, N. A.; Abdel Wahab, M. (2017b): Finite element analysis of fretting fatigue under out of phase loading conditions. *Tribology International*, vol. 109, pp. 552-562.

Bhatti, N. A.; Abdel Wahab, M. (2018): Fretting fatigue crack nucleation: a review. *Tribology International*, vol. 121, pp. 121-138.

Bhatti, N. A.; Pereira, K.; Abdel Wahab, M. (2018): A continuum damage mechanics approach for fretting fatigue under out of phase loading. *Tribology International*, vol. 117, pp. 39-51.

Bhatti, N. A.; Pereira, K.; Abdel Wahab, M. (2019): Effect of stress gradient and quadrant averaging on fretting fatigue crack initiation angle and life. *Tribology*

International, vol. 131, pp. 212-221.

Bradley, R. S. (1932): LXXIX. The cohesive force between solid surfaces and the surface energy of solids. *London, Edinburgh, and Dublin Philosophical Magazine and Journal of Science*, vol. 13, no. 86, pp. 853-862.

Bufler, H. (1959): Zur theorie der rollenden reibung. *Ingenieur Archiv*, vol. 27, pp. 137-142.

Cardoso, R. A.; Araújo, J. A.; Ferreira, J. L. A.; Castro, F. C. (2016): Crack path simulation for cylindrical contact under fretting conditions. *Frattura ed Integrità Strutturale*, vol. 10, no. 35, pp. 405-413.

Cardoso, R. A.; Doca, T.; Néron, D.; Pommier, S.; Araújo, J. A. (2019): Wear numerical assessment for partial slip fretting fatigue conditions. *Tribology International*, vol. 136, pp. 508-523.

Cattaneo, C. (1938): Sul contatto di due corpi elastici: distribuzione locale degli sforzi. *Rendiconti dell'Academia Nazionale dei Lincei*, vol. 27, no. 6, pp. 342-348.

Chakherlou, T. N.; Mirzajanzadeh, M.; Vogwell, J. (2009): Effect of hole lubrication on the fretting fatigue life of double shear lap joints: an experimental and numerical study. *Engineering Failure Analysis*, vol. 16, no. 7, pp. 2388-2399.

Conner, B. P.; Hutson, A. L.; Chambon, L. (2003): Observations of fretting fatigue micro-damage of Ti-6Al-4V. *Wear*, vol. 255, no. 1, pp. 259-268.

Conner, B. P.; Nicholas, T. (2006): Using a dovetail fixture to study fretting fatigue and fretting palliatives. *Journal of Engineering Materials and Technology*, vol. 128, no. 2, pp. 133-141.

Cotterell, B.; Rice, J. R. (1980): Slightly curved or kinked cracks. *International Journal of Fracture*, vol. 16, no. 2, pp. 155-169.

Dang Van, K.; Maitournam, M. H. (1993): Steady-state flow in classical elastoplasticity: applications to repeated rolling and sliding contact. *Journal of the Mechanics and Physics of Solids*, vol. 41, no. 11, pp. 1691-1710.

De Pannemaecker, A.; Fouvry, S.; Brochu, M; Buffiere, J. Y. (2016): Identification of the fatigue stress intensity factor threshold for different load ratios *R*: from fretting fatigue to C(T) fatigue experiments. *International Journal of Fatigue*, vol. 82, no. 2, pp. 211-225.

Deng, Q.; Bhatti, N.; Yin, X.; Abdel Wahab, M. (2018): Numerical modeling of the effect of randomly distributed inclusions on fretting fatigue-induced stress in metals. *Metals*, vol. 8, 836.

Deng, Q.; Bhatti, N. A.; Yin, X.; Abdel Wahab, M. (2020). The effect of a critical micro-void defect on fretting fatigue crack initiation in heterogeneous material using a multiscale approach. *Tribology International*, 141, 105909.

Ding, J.; Leen, S. B.; McColl, I. R. (2004): The effect of slip regime on fretting wear-induced stress evolution. *International Journal of Fatigue*, vol. 26, pp. 521-531.

Ding, J.; Sum, W.; Sabesan, R.; Leen, S.; McColl, I. et al. (2007): Fretting fatigue predictions in a complex coupling. *International Journal of Fatigue*, vol. 29, pp. 1229-1244.

Dobromirski, J. (1992): Variables of fretting process: are there 50 of them? *Standardization of Fretting Fatigue Test Methods and Equipment*, *ed. M. Attia and R. Waterhouse. ASTM International*, pp. 60-66.

Dolbow, J.; Moës, N.; Belytschko, T. (2001): An extended finite element method for modeling crack growth with frictional contact. *Computer Methods in Applied Mechanics and Engineering*, vol. 190, pp. 6825-6846.

Dubourg, M. C.; Lamacq, V. (2000): Stage II crack propagation direction determination under fretting fatigue loading: a new approach in accordance with experimental observations. *Fretting Fatigue: Current Technology and Practices*. ASTM International.

El Haddad, M. H.; Smith, K. N.; Topper, T. H. (1979): Fatigue crack propagation of short cracks. *Journal of Engineering Materials and Technology*, vol. 101, no. 1, pp. 42-46.

Endo, K.; Goto, H. (1976): Initiation and propagation of fretting fatigue cracks. *Wear*, vol. 38, no. 2, pp. 311-324.

Erdogan, F.; Sih, G. C. (1963): On the crack extension in plates under plane loading and transverse shear. *Journal of Basic Engineering*, vol. 85, no. 4, pp. 519-525.

Erena, D.; Vázquez, J.; Navarro, C.; Domínguez, J. (2018): Voids as stress relievers and a palliative in fretting. *Fatigue & Fracture of Engineering Materials & Structures*, vol. 41, no. 12, pp. 2475-2484.

Eriten, M.; Polycarpou, A. A.; Bergman, L. A. (2011): Development of a lap joint fretting apparatus. *Experimental Mechanics*, vol. 51, no. 8, pp. 1405-1419.

Faanes, S. (1995): Inclined cracks in fretting fatigue. *Engineering Fracture Mechanics*, vol. 52, no. 1, pp. 71-82.

Ferjaoui, A.; Yue, T.; Abdel Wahab, M.; Hojjati-Talemi, R. (2015): Prediction of fretting fatigue crack initiation in double lap bolted joint using continuum damage mechanics. *International Journal of Fatigue*, vol. 73, pp. 66-76.

Fleury, R.; Paynter, R.; Nowell, D. (2014): The influence of contacting Ni-based single-crystal superalloys on fretting fatigue of Ni-based polycrystalline superalloys at high temperature. *Tribology International*, vol. 76, pp. 63-72.

Forman, R. G.; Kearney, V. E.; Engle, R. M. (1967): Numerical analysis of crack propagation in cyclic-loaded structures. *Journal of Basic Engineering*, vol. 89, no. 3, pp. 459-463.

Fu, Y.; Wei, J.; Batchelor, A. W. (2000): Some considerations on the mitigation of fretting damage by the application of surface-modification technologies. *Journal of Materials Processing Technology*, vol. 99, no. 1-3, pp. 231-245.

Gandiolle, C.; Fouvry, S. (2016): Stability of critical distance approach to predict fretting fatigue cracking: a "l_{opt}-b_{opt}" concept. *International Journal of Fatigue*, vol. 82, no. 2, pp. 199-210.

Gao, Y. F.; Hu, W. B.; Wen, Z. X.; Yue, Z. F.; Chen, L. (2014): Stress field and propagation trend of crack tip in tenon of nickel-based single crystal superalloys turbine blade. *Journal of Aerospace Power*, vol. 29, no. 3, pp. 612-618.

Garg, S.; Pant, M. (2018): Meshfree methods: a comprehensive review of applications. *International Journal of Computational Methods*, vol. 15, no. 3, pp. 1830001-1-1830001-85.

Giner, E.; Díaz-Álvarez, J.; Marco, M.; Miguélez, M. H. (2015): Orientation of propagating crack paths emanating from fretting-fatigue contact problems. *Frattura ed Integrità Strutturale*, vol. 10, no. 35, pp. 285-294.

Giner, E.; Navarro, C.; Sabsabi, M.; Tur, M.; Domínguez, J. et al. (2011): Fretting fatigue life prediction using the extended finite element method. *International Journal of Mechanical Sciences*, vol. 53, no. 3, pp. 217-225.

Giner, E.; Sabsabi, M.; Fuenmayor, F. J. (2011): Calculation of K_{II} in crack face contacts using X-FEM. Application to fretting fatigue. *Engineering Fracture Mechanics*, vol. 78, no. 2, pp. 428-445.

Giner, E.; Sabsabi, M.; Ródenas, J. J.; Fuenmayor, F. J. (2014): Direction of crack propagation in a complete contact fretting fatigue problem. *International Journal of Fatigue*, vol. 58, pp. 172-180.

Giner, E.; Sukumar, N.; Denia, F. D.; Fuenmayor, F. J. (2008): Extended finite element method for fretting fatigue crack propagation. *International Journal of Solids and Structures*, vol. 45, no. 22, pp. 5675-5687.

Giner, E.; Sukumar, N.; Tarancon, T.; Fuenmayor, F. J. (2009): An Abaqus implementation of the extended finite element method. *Engineering Fracture Mechanics*, vol. 76, no. 3, pp. 347-368.

Giner, E.; Tur, M.; Vercher, A.; Fuenmayor, F. J. (2009): Numerical modelling of crack-contact interaction in 2D incomplete fretting contacts using X-FEM. *Tribology International*, vol. 42, no. 9, pp. 1269-1275.

Goh, C. H.; Wallace, J. M.; Neu, R. W.; McDowell, D. L. (2001): Polycrystal plasticity simulations of fretting fatigue. *International Journal of Fatigue*, vol. 23, pp. 423-435.

Golden, P. J. (2009): Development of a dovetail fretting fatigue fixture for turbine engine materials. *International Journal of Fatigue*, vol. 31, no. 4, pp. 620-628.

Golden, P. J.; Nicholas, T. (2005): The effect of angle on dovetail fretting experiments in Ti-6Al-4V. *Fatigue & Fracture of Engineering Materials & Structures*, vol. 28, no. 12, pp. 1169-1175.

Goldstein, R. V.; Salganik, R. L. (1974): Brittle fracture of solids with arbitrary cracks. *International Journal of Fracture*, vol. 10, no. 4, pp. 507-523.

Hamilton, G. M.; Goodman, L. E. (1966): The stress field created by a circular sliding contact. *Journal of Applied Mechanics*, vol. 33, no. 2, pp. 371-376.

Han, Q. N.; Qiu, W.; He, Z.; Su, Y.; Ma, X. et al. (2018): The effect of crystal orientation on fretting fatigue crack formation in Ni-based single-crystal superalloys: In-situ SEM observation and crystal plasticity finite element simulation. *Tribology International*, vol. 125, pp. 209-219.

Hattori, T.; Nakamura, M.; Sakata, H.; Watanabe, T. (1988): Fretting fatigue analysis using fracture mechanics. *JSME International Journal. Ser. 1, Solid Mechanics, Strength of Materials*, vol. 31, no. 1, pp. 100-107.

Hertz, H. R. (1882): Über die berührung fester elastische körper und über die harte. *Verhandlungen des Vereins zur Beförderung des Gewerbefleisses*.

Hertzberg, R. W. (1996): *Deformation and Fracture Mechanics of Engineering*

Materials, 4th edition. John Wiley & Sons, Inc.

Hills, D. A.; Dini, D. (2016): A review of the use of the asymptotic framework for quantification of fretting fatigue. *Journal of Strain Analysis*, vol. 51, no. 4, pp. 240-246.

Hills, D. A.; Nowell, D. (1994): *Mechanics of Fretting Fatigue*. Springer Science Business Media B. V.

Hills, D. A.; Nowell, D.; O'Connor, J. J. (1988): On the mechanics of fretting fatigue. *Wear*, vol. 125, no. 1-2, pp. 129-146.

Hojjati-Talemi, R. (2014): *Numerical Modelling Techniques for Fretting Fatigue Crack Initiation and Propagation (Ph.D. Thesis)*. Ghent University, Belgium.

Hojjati-Talemi, R.; Abdel Wahab, M. (2013): Fretting fatigue crack initiation lifetime predictor tool: using damage mechanics approach. *Tribology International*, vol. 60, pp. 176-186.

Hojjati-Talemi, R.; Abdel Wahab, M.; De Pauw, J.; De Baets, P. (2014): Prediction of fretting fatigue crack initiation and propagation lifetime for cylindrical contact configuration. *Tribology International*, vol. 76, pp. 73-91.

Hojjati-Talemi, R.; Abdel Wahab, M. A.; Giner, E.; Sabsabi, M. (2013): Numerical estimation of fretting fatigue lifetime using damage and fracture mechanics. *Tribology Letters*, vol. 52, pp. 11-25.

Hourlier, F.; D'Hondt, H.; Truchon, M.; Pineau, A. (1985): Fatigue crack path behavior under polymodal fatigue. *Multiaxial Fatigue*. ASTM International.

Hussain, M. A.; Pu, S. L.; Underwood, J. (1974): Strain energy release rate for a crack under combined mode I and mode II. *Fracture Analysis: Proceedings of the 1973 National Symposium on Fracture Mechanics, Part II, ed. G. Irwin*. ASTM International, pp. 2-28.

Ince, A.; Glinka, G. (2011): A modification of Morrow and Smith-Watson-Topper mean stress correction models. *Fatigue & Fracture of Engineering Materials & Structures*, vol. 34, no. 11, pp. 854-867.

Infante-García, D.; Giner, E.; Miguélez, H.; Abdel Wahab, M. (2019): Numerical analysis of the influence of micro-voids on fretting fatigue crack initiation lifetime. *Tribology International*, vol. 135, pp. 121-129.

Johnson, K. L. (1987): *Contact Mechanics*. Cambridge University Press.

Johnson, K. L.; Kendall, K.; Roberts, A. D. (1971): Surface energy and the contact of elastic solids. *Proceedings of the Royal Society A-Mathematical, Physical and Engineering Sciences*, vol. 324, no. 1558, pp. 301-313.

Kim, K.; Yoon, M. J. (2014): Fretting fatigue simulation for aluminium alloy using cohesive zone law approach. *International Journal of Mechanical Sciences*, vol. 85, pp. 30-37.

Kumar, D.; Biswas, R.; Poh, L. H.; Wahab, M. A. (2017): Fretting fatigue stress analysis in heterogeneous material using direct numerical simulations in solid mechanics. *Tribology International*, vol. 109, pp. 124-132.

Lamacq, V.; Baïetto-dubourg, M. C.; Vincent, L. (1996): Crack path prediction under

fretting fatigue-A theoretical and experimental approach. *Journal of Tribology*, vol. 118, no. 4, pp. 711-720.

Lee, H.; Mall, S. (2006): Investigation into tangential force and axial stress effects on fretting fatigue behavior. *Journal of Engineering Materials and Technology*, vol. 128, no. 2, pp. 202-209.

Li, X.; Zuo, Z.; Qin, W. (2015): A fretting related damage parameter for fretting fatigue life prediction. *International Journal of Fatigue*, vol. 73, pp. 110-118.

Llavori, I.; Zabala, A.; Urchegui, M. A.; Tato, W.; Gómez, X. (2019): A coupled crack initiation and propagation numerical procedure for combined fretting wear and fretting fatigue lifetime assessment. *Theoretical and Applied Fracture Mechanics*, vol. 101, pp. 294-305.

Lykins, C. D.; Mall, S.; Jain, V. (2000): An evaluation of parameters for predicting fretting fatigue crack initiation. *International Journal of Fatigue*, vol. 22, no. 8, pp. 703-716.

Lykins, C. D.; Mall, S.; Jain, V. (2001a): A shear stress-based parameter for fretting fatigue crack initiation. *Fatigue & Fracture of Engineering Materials & Structures*, vol. 24, no. 7, pp. 461-473.

Lykins, C. D.; Mall, S.; Jain, V. (2001b): Combined experimental-numerical investigation of fretting fatigue crack initiation. *International Journal of Fatigue*, vol. 23, no. 8, pp. 703-711.

Madge, J. J.; Leen, S. B.; Mccoll, I. R.; Shipway, P. H. (2007): Contact-evolution based prediction of fretting fatigue life: effect of slip amplitude. *Wear*, vol. 262, no. 9-10, pp. 1159-1170.

Madge, J. J.; Leen, S. B.; Shipway, P. H. (2008): A combined wear and crack nucleation-propagation methodology for fretting fatigue prediction. *International Journal of Fatigue*, vol. 30, no. 9, pp. 1509-1528.

Marco, M.; Infante-García, D.; Díaz-Álvarez, J.; Giner, E. (2019): Relevant factors affecting the direction of crack propagation in complete contact problems under fretting fatigue. *Tribology International*, vol. 131, pp. 343-352.

Martínez, J. C.; Vanegas-Useche, L. V.; Abdel Wahab, M. (2017): Numerical prediction of fretting fatigue crack trajectory in a railway axle using XFEM. *International Journal of Fatigue*, vol. 100, pp. 32-49.

McVeigh, P. A.; Farris, T. N. (1997): Finite element analysis of fretting stresses. *Journal of Tribology*, vol. 119, no. 4, pp. 797-801.

Mindlin, R. D. (1949): Compliance of elastic bodies in contact. *Journal of Applied Mechanics*, vol. 16, pp. 259-268.

Mindlin, R.; Deresiewicz, H. (1953): Elastic spheres in contact under varying oblique forces. *Journal of Applied Mechanics*, vol. 20, pp. 327-344.

Muñoz, S.; Navarro, C.; Domínguez, J. (2007): Application of fracture mechanics to estimate fretting fatigue endurance curves. *Engineering Fracture Mechanics*, vol. 74, no. 14, pp. 2168-2186.

Mutoh, Y. (1995): Mechanisms of fretting fatigue. *JSME International Journal. Ser. A, Mechanics and Material Engineering*, vol. 38, no. 4, pp. 405-415.

Mutoh, Y.; Xu, J. Q. (2003): Fracture mechanics approach to fretting fatigue and problems to be solved. *Tribology International*, vol. 36, no. 2, pp. 99-107.

Mutoh, Y.; Xu, J. Q.; Kondoh, K. (2003): Observations and analysis of fretting fatigue crack initiation and propagation. *Fretting Fatigue: Advances in Basic Understanding and Applications*. ASTM International.

Naboulsi, S.; Mall, S. (2003): Fretting fatigue crack initiation behavior using process volume approach and finite element analysis. *Tribology International*, vol. 36, no. 2, pp. 121-131.

Namjoshi, S. A.; Mall, S.; Jain, V. K.; Jin, O. (2002): Fretting fatigue crack initiation mechanism in Ti-6Al-4V. *Fatigue & Fracture of Engineering Materials & Structures*, vol. 25, no. 10, pp. 955-964.

Navarro, C.; Domínguez, J. (2004): Initiation criteria in fretting fatigue with spherical contact. *International Journal of Fatigue*, vol. 26, no. 12, pp. 1253-1262.

Navarro, C.; García, M.; Domínguez, J. (2003): A procedure for estimating the total life in fretting fatigue. *Fatigue & Fracture of Engineering Materials & Structures*, vol. 26, no. 5, pp. 459-468.

Navarro, C.; Muñoz, S.; Domínguez, J. (2006): Propagation in fretting fatigue from a surface defect. *Tribology International*, vol. 39, no. 10, pp. 1149-1157.

Navarro, C.; Muñoz, S.; Domínguez, J. (2008): On the use of multiaxial fatigue criteria for fretting fatigue life assessment. *International Journal of Fatigue*, vol. 30, no. 1, pp. 32-44.

Nix, K. J.; Lindley, T. C. (1988): The influence of relative slip range and contact material on the fretting fatigue properties of 3.5 NiCrMoV rotor steel. *Wear*, vol. 125, no. 1-2, pp. 147-162.

Noraphaiphipaksa, N.; Kanchanomai, C.; Mutoh, Y. (2013): Numerical and experimental investigations on fretting fatigue: relative slip, crack path, and fatigue life. *Engineering Fracture Mechanics*, vol. 112, pp. 58-71.

Noraphaiphipaksa, N.; Manonukul, A.; Kanchanomai, C. (2017): Fretting fatigue with cylindrical-on-flat contact: crack nucleation, crack path and fatigue life. *Materials*, vol. 10, no. 2, pp. 155.

Noraphaiphipaksa, N.; Manonukul, A.; Kanchanomai, C.; Mutoh, Y. (2014): Fretting fatigue life prediction of 316L stainless steel based on elastic-plastic fracture mechanics approach. *Tribology International*, vol. 78, pp. 84-93.

Noraphaiphipaksa, N.; Manonukul, A.; Kanchanomai, C.; Mutoh, Y. (2016): Fretting-contact-induced crack opening/closure behaviour in fretting fatigue. *International Journal of Fatigue*, vol. 88, pp. 185-196.

Nowell, D.; Hills, D. A. (1987): Mechanics of fretting fatigue tests. *International Journal of Mechanical Sciences*, vol. 29, no. 5, pp. 355-365.

Nuismer, R. J. (1975): An energy release rate criterion for mixed mode fracture. *International Journal of Fracture*, vol. 11, no. 2, pp. 245-250.

Oskouei, R. H.; Ibrahim, R. N. (2012): Improving fretting fatigue behaviour of Al 7075-T6 bolted plates using electroless Ni-P coatings. *International Journal of Fatigue*,

vol. 44, pp. 157-167.

Palaniswamy, K.; Knauss, W. G. (1978): II-On the problem of crack extension in brittle solids under general loading. *Materials Science*.

Paris, P. C.; Erdogan, F. (1963): A critical analysis of crack propagation laws. *Journal of Basic Engineering*, vol. 85, no. 4, pp. 528-533.

Paris, P. C.; Sih, G. C. (1965): Stress analysis of cracks. *Fracture Toughness Testing and its Applications*. ASTM STP 381, pp. 30-81.

Pereira, K.; Abdel Wahab, M. (2017): Fretting fatigue crack propagation lifetime prediction in cylindrical contact using an extended MTS criterion for non-proportional loading. *Tribology International*, vol. 115, pp. 525-534.

Pereira, K.; Abdel Wahab, M. (2020): Fretting fatigue lifetime estimation using a cyclic cohesive zone model. *Tribology International*, vol. 141, 105899.

Pereira, K.; Bhatti, N.; Abdel Wahab, M. (2018): Prediction of fretting fatigue crack initiation location and direction using cohesive zone model. *Tribology International*, vol. 127, pp. 245-254.

Pereira, K.; Bordas, S.; Tomar, S.; Trobec, R.; Depolli, M. et al. (2016): On the convergence of stresses in fretting fatigue. *Materials*, vol. 9, no. 8, pp. 1-15.

Pierres, E.; Baietto, M. C.; Gravouil, A.; Morales-Espejel, G. (2010): 3D two scale X-FEM crack model with interfacial frictional contact: application to fretting fatigue. *Tribology International*, vol. 43, pp. 1831-1841.

Plank, R.; Kuhn, G. (1999): Fatigue crack propagation under non-proportional mixed mode loading. *Engineering Fracture Mechanics*, vol. 62, no. 2-3, pp. 203-229.

Proudhon, H.; Fouvry, S.; Buffière, J. Y. (2005): A fretting crack initiation prediction taking into account the surface roughness and the crack nucleation process volume. *International Journal of Fatigue*, vol. 27, pp. 569-579.

Rabczuk, T.; Belytschko, T. (2004): Cracking particles: a simplified meshfree method for arbitrary evolving cracks. *International Journal for Numerical Methods in Engineering*, vol. 61, no. 13, pp. 2316-2343.

Redford, J. A.; Gueguin, M.; Nguyen, M. C.; Lieurade, H. P.; Yang, C. et al. (2019): Calibration of a numerical prediction methodology for fretting-fatigue crack initiation in overhead power lines. *International Journal of Fatigue*, vol. 124, pp. 400-410.

Ren, H.; Zhuang, X.; Rabczuk, T. (2017): Dual-horizon peridynamics: a stable solution to varying horizons. *Computer Methods in Applied Mechanics and Engineering*, vol. 318, pp. 762-782.

Ribeaucourt, R.; Baietto-Dubourg, M. C.; Gravouil, A. (2007): A new fatigue frictional contact crack propagation model with the coupled X-FEM/LATIN method. *Computer Methods in Applied Mechanics and Engineering*, vol. 196, no. 33, pp. 3230-3247.

Rozumek, D.; Macha, E. (2009): A survey of failure criteria and parameters in mixed-mode fatigue crack growth. *Materials Science*, vol. 45, no. 2, pp. 47-62.

Sato, K.; Fujii, H.; Kodama, S. (1986): Crack propagation behaviour in fretting fatigue. *Wear*, vol. 107, no. 3, pp. 245-262.

Sih, G. C. (1974): Strain-energy-density factor applied to mixed mode crack problems. *International Journal of Fracture*, vol. 10, no. 3, pp. 305-321.

Silling, S. (2000): Reformulation of elasticity theory for discontinuities and long-range forces. *Journal of the Mechanics and Physics of Solids*, vol. 48, no. 1, pp. 175-209.

Sunde, S. L.; Berto, F.; Haugen, B. (2018): Predicting fretting fatigue in engineering design. *International Journal of Fatigue*, vol. 117, pp. 314-326.

Swanson, S. R.; Cicci, F.; Hoppe, W. (1967): Crack propagation in clad 7079-T6 aluminum alloy sheet under constant and random amplitude fatigue loading. *Fatigue Crack Propagation, ed. J. Grosskreutz*. ASTM STP 415, pp. 312-362.

Szolwinski, M. P.; Farris, T. N. (1996): Mechanics of fretting fatigue crack formation. *Wear*, vol. 198, no. 1-2, pp. 93-107.

Szolwinski, M. P.; Farris, T. N. (1998): Observation, analysis and prediction of fretting fatigue in 2024-T351 aluminum alloy. *Wear*, vol. 221, no. 1, pp. 24-36.

Tur, M.; Fuenmayor, J.; Ródenas, J. J.; Giner, E. (2003): 3D analysis of the influence of specimen dimensions on fretting stresses. *Finite Elements in Analysis and Design*, vol. 39, no. 10, pp. 933-949.

Vallellano, C.; Domínguez, J.; Navarro, A. (2003): On the estimation of fatigue failure under fretting conditions using notch methodologies. *Fatigue & Fracture of Engineering Materials & Structures*, vol. 26, no. 5, pp. 469-478.

Vázquez, J.; Astorga, S.; Navarro, C.; Domínguez, J. (2016): Analysis of initial crack path in fretting fatigue. *Frattura ed Integrita Strutturale*, vol. 10, no. 37, pp. 38-45.

Vázquez, J.; Carpinteri, A.; Bohórquez, L.; Vantadori, S. (2019): Fretting fatigue investigation on Al 7075-T651 alloy: experimental, analytical and numerical analysis. *Tribology International*, vol. 135, pp. 478-487.

Vingsbo, O.; Söderberg, S. (1988): On fretting maps. *Wear*, vol. 126, no. 2, pp. 131-147.

Walvekar, A. A.; Leonard, B. D.; Sadeghi, F.; Jalalahmadi, B.; Bolander, N. (2014): An experimental study and fatigue damage model for fretting fatigue. *Tribology International*, vol. 79, pp. 183-196.

Wharton, M. H.; Taylor, D. E.; Waterhouse, R. B. (1973): Metallurgical factors in the fretting-fatigue behaviour of 70/30 brass and 0.7% carbon steel. *Wear*, vol. 23, no. 2, pp. 251-260.

Williams, J. A.; Dwyer-Joyce, R. S. (2001): *Chapter 3 Contact between Solid Surfaces*. CRC Press LLC.

Zeng, D.; Zhang, Y.; Lu, L.; Zou, L.; Zhu, S. (2019): Fretting wear and fatigue in press-fitted railway axle: a simulation study of the influence of stress relief groove. *International Journal of Fatigue*, vol. 118, pp. 225-236.

Zhang, H. Y.; Liu, J. X.; Zuo, Z. X. (2015): Numerical study of the effects of residual stress on fretting fatigue using XFEM. *Materials*, vol. 8, no. 10, pp. 7094-7105.

Zhang, H. Y.; Liu, J. X.; Zuo, Z. X. (2016): Investigation into the effects of tangential force on fretting fatigue based on XFEM. *Tribology International*, vol. 99, pp. 23-28.

Zhang, M.; McDowell, D. L.; Neu, R. W. (2009): Microstructure sensitivity of fretting

fatigue based on computational crystal plasticity. *Tribology International*, vol. 42, no. 9, pp. 1286-1296.

Zhang, Y.; Lu, L.; Gong, Y.; Zhang, J.; Zeng, D. (2017): Fretting wear-induced evolution of surface damage in press-fitted shaft. *Wear*, vol. 384-385, pp. 131-141.

Zhang, Y.; Lu, L.; Zou, L.; Zeng, D.; Zhang, J. (2018): Finite element simulation of the influence of fretting wear on fretting crack initiation in press-fitted shaft under rotating bending. *Wear*, vol. 400-401, pp. 177-183.